CLIMATE-INDUCED SURFACE WATER VARIABILITY AT MONTE SAN NICOLA TYPE-SECTION (SICILY, SOUTHERN ITALY): NEW DATA ACROSS THE GELASIAN GSSP

Marina Addante[1], Patrizia Maiorano[1*], Giovanna Scopelliti[2], Angela Girone[1], Maria Marino[1], Samanta Trotta[1], Antonio Caruso[3]

[1]Dipartimento di Scienze della Terra e Geoambientali, Università degli Studi di Bari Aldo Moro, Italy

[2]Dipartimento di Scienze della Terra e del Mare, Università di Palermo, Italy

[3]Dipartimento di Scienze e Tecnologie Biologiche, Chimiche e Farmaceutiche, Università di Palermo, Italy

Palaeogeography, Palaeoclimatology, Palaeoecology 634 (2024) 111907
https://doi.org/10.1016/j.palaeo.2023.111907

*corresponding author: patrizia.maiorano@uniba.it (P. Maiorano)

Abstract

We present the first high-resolution results on planktonic foraminifera stable oxygen isotopes and calcareous plankton assemblages at the Monte San Nicola GSSP section (Gela, Sicily), the type-section for the Lower Pleistocene Gelasian Stage. The oxygen isotope profile has a remarkable comparison with the Eastern Mediterranean oxygen isotope record and indicates that the studied section, extending from marine isotope stage (MIS) G4 to MIS 103, well records glacial-interglacial variability. Cyclic changes of calcareous plankton assemblages (calcareous nannofossils and foraminifera) indicate that warmer and stratified surface waters occurred during interglacials, while cooler and unstable conditions developed during glacial phases. Signature of further increase in surface water stratification are also captured by our surface water proxies and are coeval with enhanced monsoon run-off, developed during precession minima/insolation maxima. The surface water changes recorded at Monte San Nicola section are in phase with North Atlantic climate variability, even on suborbital scale, and reveal evidence of the first significant southward migration of the Subarctic Front in the mid-latitude during MIS 104, slightly below the GSSP. The overall dataset provides precise location of the Gelasian GSSP within MIS 103, thus improving its correlation potential outside the type-area.

Keywords: Lower Pleistocene GSSP; Mediterranean area; stable oxygen isotope; calcareous plankton; paleoclimate; North Hemisphere Glaciation

1. Introduction

The Global Boundary Stratotype Section and Point (GSSP) for the Gelasian Stage (~2.58 Ma) was formally ratified in the late nineties (Rio et al., 1998) at the Monte San Nicola section (MSNs), near Gela, in Sicily. By the time of the GSSP ratification, the Gelasian Stage represented the uppermost subdivision of the Pliocene Series, while in the following years, after several discussions within the scientific community, the base of the Quaternary was lowered from 1.8 Ma to 2.58 Ma and the Gelasian Stage was shifted into the Pleistocene (Gibbard and Head, 2010). Consequently, the Gelasian GSSP currently defines the beginning of the Quaternary System and of the Pleistocene Series (Gibbard and Head, 2010, Gibbard et al., 2010). The GSSP falls within a critical climate transition, between the end of a relatively warm climate phase, the so-called Pliocene Warm Period, at around 3 Ma, and the progressive intensification of the North Hemisphere Glaciation (iNHG), whose development begins already from 3.6 Ma, but which becomes significant around ~2.7-2.5 Ma (Mudelsee and Raymo, 2005; Westerhold et al., 2020; McClymont et al., 2023 and reference therein). The progressive ice-sheet development is supported by the widespread occurrence of Ice Rafted Debris (IRD) in North Atlantic and North Pacific sediments, starting at 2.7 Ma (Shackleton et al., 1984; Maslin et al., 1998; Kleiven et al., 2002; Naafs et al., 2012) and by the $\delta^{18}O$ enrichment of deep-sea benthic isotope records, suggesting a global impact of increasing ice volume (Tiedemann et al., 1994; Shackleton et al., 1995; Lisiecki and Raymo, 2005; Westerhold et al., 2020). During this climate transition, Marine Isotope Stage (MIS) 100 is known as the first full glacial cycle and one of the first pronounced obliquity-controlled glacial periods (Shackleton et al., 1984; Raymo et al., 1989). In the North Atlantic, a significant reorganization in the hydrologic dynamic is known to have started at ~2.6 Ma, mostly based on evidence from dinoflagellate cysts and planktonic foraminifera assemblage (Hennissen et al., 2014; Bolton et al., 2018), indicating that the first significant southward shift of the North Atlantic Current and of the Subarctic Front occurred during MIS 104. In the central and eastern Mediterranean evidence of the polar influence have been suggested at MIS 110 (Zachariasse et al., 1990; Lourens et al., 1992, 1996; Becker et al., 2005), although a correlation with Atlantic records was not provided. A large set of proxies has been applied to different records to reconstruct climate evolution, suggesting that the iNHG was rather complex in terms of ice-sheet advances/retreats and non-uniform on a global scale (McClymont et al., 2023 and references therein). Despite the chronostratigraphic relevance of the MSN sedimentary record and the importance of the climate transition embedded across the Gelasian GSSP, the type-section (MSNt-s) has not been studied with a high-temporal resolution detail since its ratification to date. No planktonic oxygen isotope record is currently available through the section. Concerning calcareous plankton studies,

most of the works were carried out until the end of the nineties (Spaak, 1983; Driever, 1988; Channell et al., 1992; Sprovieri, 1992, 1993; Rio et al., 1994, 1998), and mostly focused on biostratigraphy and based on multi-millennial resolution. From a climatostratigraphic point of view, the last work dates to Rio et al. (1998), which includes a low-resolution record of *Globigerinoides* abundance fluctuations employed as proxy for glacial/interglacial stages. A single paper has provided a centennial-scale climate reconstruction in the type-area (Becker et al., 2005), although focusing on a brief portion of the sedimentary record and specifically the MIS 101-MIS 99 interval. More recently, a new stratigraphic profile has been investigated nearby the MSNt-s, named "Mandorlo" section (Capraro et al., 2022), mainly targeting on bio- and magnetostratigraphic issues and with the intention to propose a potential-unit stratotype of the Gelasian Stage. Considering this lack of knowledge, we present the first high-resolution results focused on the surface water variability signals embedded in the MSNt-s. Our proxies consist of planktonic stable oxygen isotopes and calcareous plankton assemblages. We focus on the reconstruction of the surface water variability recorded in the type-section between ~2.7 and 2.5 Ma, on its relationship with orbital forcings and correlation with extra-Mediterranean records. The results enable to frame the section within the climate evolution at the Pliocene-Pleistocene transition and strengthen the correlation potential of the MSNt-s and of the GSSP itself outside the type-area.

2. Materials and methods

2.1 Monte San Nicola section and the study interval

The MSNt-s, located few km NW of Gela (Sicily), outcrops in the southeastern part of the Caltanissetta sedimentary basin (Sicily), a late Neogene structure located between the Sicilian-Maghrebian Chain and the Hyblean Foreland (Fig. 1A-B) (Catalano et al., 2013; Lentini and Carbone, 2014). The Plio-Pleistocene sediments in the basin represent the final filling of a piggy-back basin of the appeninic-maghrebid chain on the Gela Nappe (Ogniben, 1969), an allochthonous unit that overthrusts the intensely deformed Cretaceous-Eocene "Argille Scagliose" (Ogniben, 1969) and the Lower Miocene "Flysch Numidico" (Gasparo Morticelli et al., 2015; Pinter et al., 2016, 2018). The whole section, originally studied by Channel et al. (1992), Rio et al. (1994; 1998), consists of a basal portion of rhythmically bedded marly limestones and marls, about 36m thick, belonging to the Zanclean-Piacenzian p.p. Trubi Formation (Cita and Gartner, 1973), passing upward to the Piacenzian p.p.- Calabrian p.p marly-silts of the Monte Narbone Formation. The younger portion is about 125m thick and includes a spectacular record of brownish-red laminated intervals, representing the

Mediterranean Precession-related Sapropels (MPRS). These layers were used for constructing the Astronomical Time Scale (ATS) of the late Neogene (Hilgen, 1991a, 1991b; Hilgen and Krijgsman, 1999). The type-section includes the clusters of sapropels O-A-B-C (Verhallen, 1987; Zijderveld et al., 1991) (Fig. 1C) and was deposited in a slope-basin setting with water depth ranging between 500-1000m (Rio et al., 1994).

For the present study, a continuous and undisturbed section, about 9m thick, belonging to the Monte Narbone Fm, was investigated (Fig. 1D). The interval mainly consists of massive whitish marls (average thickness of ~135cm) alternated to slightly dark gray bioturbated marly clays (average thickness of ~31cm), namely sapropel layers A2 to A4/5. Bioturbation is mainly represented by *Chondrites* ichsp., *Planolites* ichsp., and *Thalassinoides* ichsp. In the upper part, the section includes a laminated clayey silts layer (35cm thick), bearing a reddish-brown surface alteration. It is the sapropel A5, which represents the topmost of cluster A, the so-called Nicola Bed, related to i-cycle 250. The Gelasian GSSP is located at the base of the marls overlying the Nicola Bed, whose midpoint has an astrochronological age of 2.588 Ma (Lourens et al., 1996, 1998), and falls within the interglacial stage MIS 103 based on *Glodigerinodes* spp. abundance fluctuations and correlation with oxygen isotope profile at Singa section (Lourens et al., 1992; Rio et al., 1994, 1998). The age of the GSSP was assumed as 2.588 Ma (Rio et al., 1998) or ~2.58 Ma, i.e. about 3.5–5.0 kyr younger than the midpoint age (Head, 2019 and reference therein).

After cleaning the weathered surface, sampling was performed every 5cm which, based on the estimated sedimentation rates (~8cm/kyr), allows a centennial-scale resolution (~800 years). The presence of MPRS and their correlation with the insolation cycles provide a precise chronological control of the succession.

2.2 Stable isotope analyses

The stable oxygen isotope analyses were carried out on 6–8 tests of the planktonic foraminifer *Globigerina bulloides* handpicked from 168 samples. The shells were selected from the fraction 150μm and carefully cleaned to remove clay and detritus from the inner parts of the chambers. In detail, following Quintana Krupinski et al. (2017), the tests were crushed using two glass slides under the stereo microscope and then cleaned by three washing cycles (30 s each) with 500μl of methanol in an ultrasonic bath. The residual methanol was extracted and, after a last ultrasonic wash with 500μl of deionized water, samples were dried before the analyses. The $\delta^{18}O$ measurement was carried out by a Thermo Scientific Delta V Advantage continuous flow IRMS equipped by an automated

Carbonate Preparation Device (Thermo Scientific GasBench II) at the Department of Scienze della Terra e del Mare of the University of Palermo (Sicily, Italy). Every 20 samples, the NBS19 international standard ($\delta^{18}O_{V\text{-}PDB}$ = -2.20‰) was run. An internal laboratory standard (Carrara Marble with $\delta^{18}O_{V\text{-}PDB}$ = -2.43‰) was also measured every 10 samples and the repeatability precision (σ) was day-to-day calculated on the replicate measurements, being always better than 0.09‰.

2.3 Calcareous plankton analyses

A total of 171 samples were analyzed for calcareous nannofossil investigations. Slides were prepared following the technique of Flores and Sierro (1997) and analyzed under a polarized light microscope at 1000x magnification at the Dipartimento di Scienze della Terra e Geoambientali (Bari, Italy). Abundances were determined by counting at least 300 coccoliths of all sizes. For specimens of the genus *Discoaster*, given their rarity and their stratigraphic utility, the count was extended up to 100 fields of view. The taxonomic identification was made at the species and subspecies level, following Young et al. (2003) and Jordan et al. (2004). The N ratio index was calculated according to Flores et al. (2000), following the ratio: small placoliths/(small placoliths + *Florisphaera profunda*). Small placoliths (< 3μm) include small *Gephyrocapsa* and small *Reticulofenestra*. High values in the N index (values closer to 1) indicate upwelling and shallow nutricline/thermocline position, while low values (values closer to 0) imply weak upwelling and relatively deep nutricline/thermocline position.

Quantitative analyses of planktonic foraminifera assemblages were performed on 92 samples with a temporal resolution of about one sample every 1000-1500 years. The samples were dried and washed on a 63μm sieve, and the residue greater than 125μm was used to obtain the quantitative abundances of taxa. The residues were split until a representative aliquot containing about 250/300 specimens has been obtained. All specimens were counted in the aliquots and species abundances were quantified as percentages on the total number of planktonic foraminifera.
Different morphotypes of *Globigerinoides ruber* were identified using the morphotype concepts of Wang (2000), Aurahs et al. (2011) and Bonfardeci et al. (2018). *Trilobatus sacculifer* includes *Trilobatus trilobus* and *Trilobatus quadrilobatus* (sensu Hemleben et al., 1989; André et al., 2013; Spezzaferri et al., 2015). *Neogloboquadrina incompta* corresponds to those specimens previously referred to as *Neogloboquadrina pachyderma* (dextral) and includes intergradations between *N. pachyderma* (dextral) and *Neogloboquadrina dutertrei* (Darling et al., 2006). *Neogloboquadrina atlantica* includes dextral and sinistral coiling specimens.

Principal Component Analysis (PCA) was performed on the percentage abundance of the assemblages using the software PAST (PAleontologySTatistic) (Hammer and Harper, 2001), to understand the main control factors that influenced distribution and abundance of taxa. For the foraminifera assemblage the involved dataset contains percentage in abundance of all the taxa with respect to the total foraminifera assemblages. For calcareous nannofossils, PCA analysis was carried out according to Aitchison (1981, 1986), a valuable method to remove effects of the constant-sumconstraint (CSC). This procedure allows to amplify the importance of less abundant species and minimize the dominance of few abundant taxa.

2.4 Chronology

Our age model was constructed by tuning each sapropel midpoint to insolation maxima, using the numerical solution of Laskar et al. (2004) for the summer season (June – July) at 65° N. We did not introduce a 3-ky lag between African monsoon maxima and insolation maxima (Lourens et al., 1996; Ziegler et al., 2010; Konijnendijk et al., 2014). This follows recent high-resolution oxygen isotope chronology developed in the Mediterranean area (Grant et al., 2022) and based on the hypothesis that the late Pliocene and Early Pleistocene sapropels were directly in-phase with precession minima/insolation maxima (Lourens et al., 2001). A cubic spline function was then used for dating all the sampling points to reduce loss of amplitudes at higher frequencies and reduced bias effect (Schulz and Statteger, 1997; Ziegler et al., 2010; Konijnendijk et al., 2014). An identical approach for the age model construction was used for the Punta Piccola reference section (Sprovieri et al., 2006), where the Piacenzian GSSP was defined (Castradori et al., 1998), and in which the entire Piacenzian stratotype, including the A1-A5 sapropels, occurs (Hilgen, 1991a; Lourens et al., 1996; Sprovieri et al., 2006). Based on the constructed chronology the studied interval extends from 2.7 to 2.57 Ma.

3. Results

3.1 Oxygen isotopes

The MSNt-s $\delta^{18}O$ depth-profile shows discrete fluctuations around an average value of 0.90‰ (Fig. 2). Prominent excursions towards negative ratios (evidenced in red in Figure 2) are related to the five sapropels included in the studied interval. In the lower part of the section, two negative $\delta^{18}O$ values (-0.63 and -0.50‰, respectively) mark the top of the sapropels A2 and A3. Sapropel A4 is well defined by three negative excursions (the most negative of -0.59‰), while the lowest $\delta^{18}O$ ratios within the

whole section characterize the base of sapropels A4/5 and A5 (-1.94 and -1.88‰, respectively). The only negative peak (-0.44‰) which does not correspond to a sapropel layer is recorded at 720cm, between sapropels A4/5 and A5. As for the heaviest oxygen isotope ratios recorded in the MSNt-s, they are located in three intervals (marked in blue in figure 2), at 10–130, 385–460 and 690–705cm, respectively. Moreover, the average $\delta^{18}O$ value calculated for each of the three intervals is progressively more positive from the base to the top of the section (1.67‰, 1.73‰, 1.98‰, respectively).

3.2 Calcareous plankton assemblage

3.2.1 Calcareous nannofossils

A total of fifty calcareous nannofossil taxa at level of genus, species and subspecies have been identified. A good coccolith preservation is generally recorded along the section, with rare evidence of slight dissolution mainly observed within sapropel layers. The overall composition of the assemblage is provided in Figure 2 and expressed in % abundances, while the abundance of climate-sensitive taxa is shown individually, in more detail, below. The genus *Reticulofenestra* including *Reticulofenestra* spp. < 3µm, *Reticulofenestra* spp. 3-5µm and *Reticulofenestra* spp. 5-7µm, represents the main component, with values ranging from 18% to 71%. The genus has several fluctuations although not distinctly correlated with the $\delta^{18}O_{G.\ bulloides}$ record. Small *Gephyrocapsa* spp. (< 3µm) are also an important component of the assemblage with abundances ranging between 3% to 47% and highest percentages up to sapropel A4. Relative abundances of *Calcidiscus* spp. (*Calcidiscus leptoporus* ssp. small, *C. leptoporus* ssp. *leptoporus*; *C. leptoporus* ssp. *quadriperforatus*, *Calcidiscus macintyrei*) ranges from 2% to 20%, while abundance of *Florisphaera profunda* varies between 0 and 17%, reaching the highest percentages within sapropel layers and particularly during sapropel A5. A similar distribution is observed for *Helicosphaera sellii*, reaching values up to 8% during sapropel A5. Highest abundance (7%) during sapropel A5 are also observed for *Helicosphaera carteri. Coccolithus pelagicus* (1-12%) is mainly represented by *Coccolithus pelagicus* ssp. *pelagicus*, although few specimens of C. *pelagicus* ssp. *braarudii* and *C. pelagicus* ssp. *azorinus* were also recorded. *Umbilicosphaera jafari* shows similar values recording the highest abundances (12%) in correspondence of the uppermost heaviest values of $\delta^{18}O_{G.\ bulloides}$ record. Taxa with subordinate abundance include *Discoaster* spp. and *Syracosphaera* spp. (*S. pulchra*+*S. histrica*), which never exceed 3% and *Rhabdosphaera* spp. (*R. clavigera* and *R. stylifera*), showing values up to 2%. “Other taxa” include all the taxa having rare and/or scattered occurrences and specifically

Pseudoemiliania lacunosa, *Helicosphaera* spp., *H. wallichii, Calciosolenia* spp., *Coronosphaera* spp., *C. mediterranea*, *Umbilicosphaera sibogae*, *U. rotula*, *U. foliosa, Pontosphaera* spp., *Scyphosphaera* spp., *Discosphaera tubifera*, *Umbellosphaera* spp. and holococcoliths. From a biostratigraphic point of view, the continuous occurrence of *Discoaster pentaradiatus*, *D. surculus* and *D. brouweri* indicates that the whole interval falls within the *D. pentaradiatus* biozone – MNN16b/17 (Rio et al., 1990) (Fig. 2).

3.2.2 Planktonic foraminifera

Planktonic foraminifera are well preserved and diversified at the MSNt-s. In the samples collected within the sapropel layers, pyrite is identified under microscope mainly as infill in foraminiferal tests or steinkerns. A total of sixteen taxa has been recognized at level of species and species-group. The foraminifera assemblage (Fig. 2) is dominated by *Globigerina bulloides*, *Globigerinita glutinata* and *Turborotalita quinqueloba* that all together represent more than 60-65% during the phases of heaviest oxygen isotope ratio. During the phase of depletion of $\delta^{18}O_{G.bulloides}$ record, *G. ruber* group shows the highest abundance values and *Neogloboquadrina acostaensis* and *Globorotalia crassaformis* are important common component of the assemblages. *Trilobatus sacculifer* and *Globigerinoides obliquus extremus* show sharp increases during the highest depletion of the $\delta^{18}O$ record corresponding to the sapropels, while *Globorotalia bononiensis* occurs along the entire studied interval. In the "others" are grouped all the taxa with rare and/or scattered occurrences including *Neogloboquadrina dutertrei*, *N. incompta*, *Globorotalia scitula*, *Orbulina universa*, *Globigerinella siphonifera*. *Neogloboquadrina atlantica* has a very scattered distribution showing a short and sharp increasing in correspondence of the heaviest values of $\delta^{18}O_{G.bulloides}$ record at ~ 700cm. The absence of *Sphaeroidinellopsis seminulina* and the occurrence of *G. bononiensis* indicate that the studied interval falls within the Subzone MPL5a (Lirer et al., 2019).

4. Discussion

4.1 Framing MSNt-s $\delta^{18}O$ record within a high-resolution Mediterranean context

The high-resolution dataset provided for the MSNt-s allows to investigate in detail changes of the surface water structure recorded between ~ 2.7 and 2.5 Ma. Before using the measured $\delta^{18}O_{G.bulloides}$ ratios in terms of regional and global climatic changes, it is however essential to evaluate the quality

of dataset and the efficiency of the shell cleaning method, although extensively tested in similar studies (e.g., Howell et al., 1998; Grant et al., 2022). To this purpose, the isotope composition measured in the MSNt-s was compared with the $\delta^{18}O$ data available for the same interval in the Mediterranean area. In particular, the box-and-whisker plot of Figure 3 summarizes the $\delta^{18}O_{G.bulloides/G.ruber}$ data from: two low-resolution records i.e. ODP Site 964 (Howell et al., 1998) and Singa section (Lourens et al., 1992), and a high-resolution dataset from the Eastern Mediterranean i.e. ODP Site 967 (Grant et al., 2022). As shown, the median of oxygen isotope composition measured on *G. bulloides* in the MSNt-s fits well with the homologue from Site 964, while the medians of $\delta^{18}O$ determined on *G. ruber* are about 2‰ lighter. According to Mulitza et al. (2022), the $\delta^{18}O_{G.ruber}$ can be until 3‰ lower than the $\delta^{18}O_{G.bulloides}$ as consequence of species-specific variability. Finally, the greater extension of the lower whisker in the MSNt-s and in Site 967 is probably related to the higher resolution of these datasets, which allow to record the full variability in the isotopic signal.

The reliability of our oxygen isotope data is further confirmed by the remarkable comparison with the high-resolution Eastern Mediterranean oxygen isotope planktonic record recently published by Grant et al. (2022; Fig. 4). The Eastern Mediterranean curve provides a valuable reference record for interpreting the $\delta^{18}O$ profile and framing the MSNt-s within a chronological and climate Mediterranean context. Thanks to the occurrence of the chronologically well constrained MPRS, the three intervals of heavier $\delta^{18}O$ phases recorded in MSNt-s can be correlated to MIS G4, G2 and 104, while lighter values capture MIS G3, 105 and 103, where the GSSP is located. Glacial cooling seems to intensify within MIS 104, where the heaviest $\delta^{18}O$ values are recorded, similarly to the Eastern Mediterranean record, suggesting that a change in Mediterranean surface water properties developed slightly below the GSSP.

Superimposed to glacial-interglacial variability, larger amplitude $\delta^{18}O$ excursions, ranging between 1-4‰, clearly occur in our record, nearly coincident with sapropel layers. This pattern is in very good concordance with the Eastern Mediterranean record (Fig. 4) and is related to major influx of low-$\delta^{18}O$ freshwater into the eastern Mediterranean (e.g. Kallel et al., 2000; Emeis et al., 2000a, 2000b, 2003), due to African river-runoff and circum-Mediterranean humidity discharge, during maximum intensity of the African monsoons triggered by northern Hemisphere summer insolation maxima (Rossignol-Strick et al., 1982; Jenkins and Williams, 1984; Rohling and Hilgen, 1991; Béthoux, 1993; Rohling, 1994; Rohling and Pälike, 2005; Grant et al., 2016). This evidence, combined with the correlation with the orbital parameters (Fig. 5), clearly indicate that the MSNt-s $\delta^{18}O$ record reflects both obliquity-forced glacial-interglacial variability, and regional precession-related temperature and salinity changes. Significant $\delta^{18}O$ excursions are also noted within sapropel A4 and A5 (Fig. 4),

suggesting the occurrence of multicentennial-scale variability accompanying the sapropel deposition. Although this issue is beyond the focus of the present paper, it is noteworthy that similar high-frequency variability was observed during the Holocene sapropel S1 and related to solar-driven precipitation changes within the Mediterranean (i.e. Jilbert et al., 2010; Hennekam et al., 2014; Maiorano et al., 2019).

4.2 Calcareous plankton and surface water variability

Data on the contribution of calcareous nannofossils for unraveling climate variability through the investigated interval in the Mediterranean area are rather scarce, while few information is available from extra-Mediterranean records (Gibbs et al., 2004; Bolton et al., 2010; Tangunan et al., 2018). On the contrary, the foraminifera assemblages have been extensively applied in the paleoclimate studies through the investigated interval in Mediterranean records (e.g. Lourens et al., 1992, 1996; Caruso, 2004; Becker et al., 2005; Sprovieri et al., 2006).

Considering that the late Pliocene nannofossil assemblage is made up of several extinct taxa, whose ecological behavior is not clearly documented, we performed a Principal Component Analyses (PCA) to identify the main environmental control on abundance and distribution of the nannofossil taxa and compare the response with the $\delta^{18}O$ record.

The results of PCA nanno yields the first components (PC1) with 21% of the variance. The most relevant taxa for each component are indicated in Table 1. Taxa with higher positive loadings are *Discoaster* spp., *C. leptoporus* ssp. small, *C. leptoporus* ssp. *leptoporus*, *Florisphaera profunda*, *Helicosphaera sellii*. Negative loadings are recorded for *Syracosphaera* spp., *Rhabdosphaera* spp., *Umbilicosphaera jafari* and *Calcidiscus* ssp. *quadriperforatus*.

The PCA has been also applied to planktonic foraminifera assemblages to further unravel the observed changes in the abundance patterns. The first two factors that explain 36% and 26% have been interpreted and discussed. The $PC1_{forams}$ gives the highest negative component loadings (Table 2) for *Neogloboquadrina acostaensis* and *N. dutertrei* together with *G. obliquus extremus* and *G. ruber* group, while it positively loads *G. glutinata*, *G. bulloides* and *T. quinqueloba*. In $PC2_{forams}$, *G. bulloides* has positive loadings and *G. glutinata* contributes negatively (Table 2).

4.3 Environmental forcing factors

Regarding the calcareous nannofossil assemblage we suggest that the first component ($PCA1_{nanno}$) (Fig. 5, Table 1) discriminates between taxa preferring warmer and stratified surface waters (positive values) and assemblage taking advantage from cooler and unstable environment. In fact, discoasterids are known to represent a k-selected group, having affinity for warm, deep photic water and stable environments (Haq, 1980; Lohmann and Carlson, 1981; Flores and Sierro, 1987; Chepstow-Lusty et al., 1989; Aubry, 1992; Chepstow-Lusty et al., 1992; Flores et al., 1992, 1995; Young, 1998; Vázquez et al., 2000). It has also been suggested that the extinct *Discoaster* genus had a habitat like that of the living *F. profunda,* increasing in abundance with deep pycnocline (Flores et al., 2005). Indeed *F. profunda*, which loads positively as discoasterids, is a deep dweller photic zone taxon of the tropical and subtropical oceans, sensitive to temperature > 10°C and reaching high abundance related to warm waters and to the occurrence of a deep nutricline (Okada and Honjo, 1973; Molfino and McIntyre, 1990; Beaufort et al., 1997; Okada and Wells, 1997). *Calcidiscus leptoporus* ssp. *leptoporus* is considered by several authors as being characteristic of tropical to subtropical oligotrophic warm-water masses (McIntyre and Bé, 1967; Okada and Honjo, 1973; Kleijne, 1993), or an indicator for periods of lower productivity and a member of a typical transitional assemblage, from colder to warmer coccolithophore communities (Silva et al., 2008). The smaller morphotype has been considered to have preference for warmer waters in Atlantic Ocean (Boeckel and Baumann, 2008) and Mediterranean Sea (Trotta et al., 2022). *Helicosphaera sellii* is an extinct taxon that has been related to deeper warmer waters (Triantaphyllou et al., 1999; Farouk et al., 2021). Therefore, the taxa bearing positive loadings share a preference for warm and stratified surface waters. About those taxa recording negative loadings, it seems clear that they share a preference for unstable surface water conditions. Although the ecology of the extinct *Umbilicosphaera jafari* is not very well understood, its peaks in abundance in few Mediterranean sedimentary records have been observed in coincidence with strong variations in the $\delta^{18}O$ isotope record, related to an increase in evaporation/precipitation ratio (Flores et al., 2005). The taxon has been proposed to have the ability to flourish in shallow water, hypersaline environments (Flores et al., 2005; Wade and Bown, 2006). Among *Calcidiscus* spp., *C. leptoprus* ssp. *quadriperforatus* is considered to have a more opportunistic behavior than *C. leptoporus* ssp. *leptoporus* (e.g. Haidar and Thierstein, 2001; Renaud et al., 2002; Silva et al., 2009) and more suitable to take advantage of more productive environments (Silva et al., 2013). Concerning *Syracosphaera* spp. and *Rhabdosphaera* spp., the increased abundance of these taxa within the Mediterranean Sea has been related to enhanced detrital input and turbid waters (Weaver and Pujol, 1988; Colmenero-Hidalgo et al., 2004; Maiorano et al., 2013, 2016), and related to abrupt millennial-

scale events during glacials (Colmenero-Hidalgo et al., 2004; Maiorano et al., 2016; Marino et al., 2018). The positive loadings of both *U. jafari* and *C. leptoprus* ssp. *quadriperforatus* in the first component seems to suggest a similar opportunistic behavior of these taxa, likely related to unstable conditions in surface waters.

$PC1_{forams}$ (Fig. 5) negatively groups species whose distribution is mainly controlled by food availability in the water column (the extinct *Neogloboquadrina acostaensis* and the still living *N. dutertrei*) with species (*G. obliquus extremus* and *G. ruber*) that flourish in oligotrophic, warm and well stratified waters (Bé and Hamlin, 1967; Bé and Tolderlund, 1971; Bé et al., 1971; Loubere and Moss, 1986; Hemleben et al., 1989; Dowsett and Poore, 1990; Caruso, 2004; Sprovieri et al., 2006) (Table 2). Considering that *N. dutertrei* is generally distributed in tropical to temperate regions and that it is abundant in the stratified mixed layer where DCM is well developed (Fairbanks et al., 1980; Fairbanks and Wiebe, 1980; Watkins et al., 1996; Watkins and Mix, 1998; Schmuker and Schiebel, 2002), negative values seem to indicate warm and stratified conditions of water column. Positive loadings discriminate an association characterized by high productivity-related taxa such as *G. glutinata* and *G. bullloides* and cool water taxa such as *T. quinqueloba* and, although with a small contribution, the subpolar cold species *N. atlantica* (Berggren, 1972; Poore and Berggren, 1975; Dowsett and Poore, 1990; Zachariasse et al., 1990; Dowsett and Robinson, 2007) (Table 2). It is known that *G. glutinata* is a high productivity-related taxon, both at low and high latitudes (Bé and Tolderlund, 1971; Thunell and Reynolds, 1984; Hemleben et al., 1989) and proliferates under conditions of strong deep winter mixing (Munz et al., 2015), while *G. bulloides* is an opportunistic species thriving in eutrophic setting related to upwelling, strong seasonal mixing or river input (Tolderlund and Bé, 1971; Pujol and Grazzini, 1995; Rohling et al., 1997; Bárcena et al., 2004; Geraga et al., 2005, 2008). *T. quinqueloba* is a typical species of the transitional to subpolar provinces in the North Atlantic and is the most abundant t axon in cool surface waters (Tolderlund and Bé, 1971; Bé, 1977; Hemleben et al., 1989), with temperature ranging from 2.2 °C to 16 °C and an optimum between 4.6 °C and 10.8 °C. Based on these considerations $PC1_{forams}$ seems to reflect mainly variations in sea surface temperature discriminating an association indicative of warm and stratified conditions (negative values) by an association indicative of cool and eutrophicated waters.

The patterns of the $PC1_{nanno}$ and $PC1_{forams}$ reveal that the abundance and distribution of calcareous plankton mainly reflect cyclic changes in temperature and stability/stratification of surface water (Fig. 5). $PC1_{nanno}$ and $PC1_{forams}$ strongly co-vary with the MSNt-s $\delta^{18}O$ record, as evidenced by concomitant changes associated with obliquity-forced glacial-interglacial phases. Warmer and stratified surface

waters are recorded during interglacials, while cooler and unstable conditions characterize glacial phases. An additional calcareous nannofossil proxy, i.e. the N ratio (Flores et al., 2000), which relies on the abundance of dominant small placoliths and of *F. profunda,* has been also considered for reconstructing nutricline depth variations (Fig. 5). Phases of relatively deeper nutricline occur during interglacials and agree with a stable-stratified column water, thus supporting our reconstruction based on PCA. A higher frequency variability is also observed during interglacials, more clearly visible in the indices of calcareous plankton (Fig. 5). Three warmer phases occur during G3 and G1, likely related to both obliquity and insolation maxima, thus suggesting a strong orbital control on calcareous plankton distribution in the studied section. On the other hand, maximum nutricline depth is recorded during sapropel A5, which is associated with stronger Northern Hemisphere summer insolation, during precession minimum and maximum obliquity (Fig. 5). This astronomical configuration was likely responsible for heavier precipitation due to the strengthening of the North African monsoon circulation (Bosmans et al., 2015) and consequent enhanced sea surface water stratification. The strong increase in the abundance of *H. carteri*, during sapropel A5 (Fig. 5), seems to reflect the highest insolation maximum correlated to i-cycle 250. Indeed the taxon is known to benefit from turbid upper water layer (Colmenero-Hidalgo et al., 2004; Bonomo et al., 2014, 2021; Maiorano et al., 2019; 2021) likely resulting from the consequent enhanced monsoon-related discharge at the site location. A very good concordance is observed between our biotic indices and $\delta^{18}O$ record at the MSN, and the lower resolution alkenone-based Mediterranean SST record (Herbert et al., 2015, 2018) (Fig. 5), supporting the validity of our proxies as indicative of Mediterranean surface water temperature variability. Finally, minimum values of $PCA1_{nanno}$, coupled with the heaviest values in $\delta^{18}O$ record, highlights a disturbance in surface waters during MIS104, which is discussed in more details below.

4.4 Precessional forcings on the calcareous plankton assemblage

Looking in more details at the patterns of three key calcareous nannofosssil taxa, which are shown individually in Figure 6, a visual correlation with insolation/precession is clearly observed. As expected, this is evident for the pattern of *F. profunda,* as a result of its well-known relation with stratified surface waters and DCM development (Rohling and Gieskes, 1989; Castradori, 1992; Kemp et al., 1999; Negri et al., 1999; Negri and Giunta, 2001; Corselli et al., 2002; Thomson et al., 2004; Triantaphyllou et al., 2010; Incarbona et al., 2011; Grelaud et al., 2012; Incarbona and Di Stefano, 2019; Maiorano et al., 2019) occurring during precession minima/insolation maxima (Hilgen, 1991a; Lourens et al., 1996) and due to intensified monsoon freshwater release especially *via* Nile River

(Rossignol-Strick et al., 1982; Rohling et al., 2002; Marino et al., 2009; Weldeab et al., 2014; Hennekam et al., 2015). Interestingly, new evidence is here observed for the taxa *H. sellii* and *C. pelagicus* ssp. *pelagicus*, whose relationship with orbital forcing in the Mediterranean was not documented so far. In the study record, *H. sellii* increases during insolation maxima/precession minima (Fig. 6), similarly to *F. profunda*, thus highlighting a comparable orbital relation for warm, stratified surface waters developed during monsoon run-off increase. The positive relation of both the taxa with precession-related humidity increase is supported by the correlation of the abundance peaks of *F. profunda* and *H. sellii* with increases in the monsoon-related African run-off proxy (Grant et al., 2017) (Fig. 6). Conversely, *C. pelagicus* ssp. *pelagicus* clearly increases during summer insolation minima/precession maxima, likely in relation to cooler environment and thermocline shift/shallowing on a precessional timescale. The living C. *pelagicus* ssp. *pelagicus* is considered a subarctic taxon (Baumann et al., 2000; Geisen et al., 2002). The taxon is known to have modified biogeographic distribution through the late Cenozoic, showing a drastic drop in abundance in the low- and mid-latitude at the Pliocene-Pleistocene transition (McIntyre and Bé, 1967; Raffi and Rio, 1981; Backman, 1984; Sato et al., 2004). In the Pliocene fossil record its ecological requirement is not investigated in detail, although a preference for cool waters has been inferred in both Mediterranean (Raffi and Rio, 1981) and extra-Mediterranean area (Bolton et al., 2010; Tangunan et al., 2018). Based on rare high-resolution data, the relationship of the taxon with precessional forcing has been also pointed out in the late Pliocene from low-latitude deep-sea ocean records (Bolton et al., 2010) and is well supported by the present results at the MSNt-s in the Mediterranean area. The cyclic *C. pelagicus* ssp. *pelagicus* fluctuations recorded in the MSNt-s appear also well related with the wet-dry index proxy (Grant et al., 2017) (Fig. 6), indicating increase of the taxon during drier phases likely in relation with cooler, mixed surface water environment during insolation minimum. Considering the strong relation of the three considered calcareous nannofossil taxa with insolation/precession forcing, we propose the use of the ratio (*F. profunda* + *H. sellii)*/(*F. profunda* + *H. sellii* + *C. pelagicus* ssp. *pelagicus*) to track, in the study section, the precession-related variations of thermocline/nutricline depth. High values of the ratio are interpreted as deep thermocline/nutricline conditions, developing during precession minima/insolation maxima, while lower values capture cooler/shallower thermocline phases, established in relation with precession maxima/insolation minima. The pattern of $PC2_{forams}$ gives additional support to this climate framework. The cosmopolitan mixed-layer species *G. glutinata* (Bé et al., 1985), which contributes negatively, is also a common component in productivity coastal and open-ocean upwelling areas (Hemleben et al., 1989; Naidu and Malmgren, 1996; Munz et al., 2015). In contrast, *G. bulloides*, due to its opportunistic behavior, has been used as an indicator of high-nutrient content in relations to strong seasonal mixing or river input (Tolderlund and Bé, 1971;

Hemleben et al., 1989; Pujol and Grazzini, 1995; Rohling et al., 1997; Bárcena et al., 2004; Geraga et al., 2005, 2008). In the Mediterranean, high abundances of *G. bulloides* during the depositions of sapropel layers have been attributed to the increased riverine input in the surficial waters (Rohling et al., 1997; Zachariasse et al., 1997; Geraga et al., 2005, 2008, 2010). Positive values of $PC2_{forams}$ correlate with insolation maxima (Fig. 6) and can thus be interpreted as an additional signal of monsoon run-off at the studied location. The positive correlation with the proxy developed in the eastern Mediterranean supports this hypothesis (Fig. 6).

4.5 First signal in the Mediterranean Sea of southward migration of the Subarctic Front and evidence of Mediterranean – Atlantic climate connection in the Gelasian MSNt-s

The heaviest $\delta^{18}O$ value of 2.4‰ is recorded at 2606 ka, during MIS 104. This shift is concurrent with a marked change observed in the distribution of *Neogloboquadrina atlantica* in the planktonic foraminifera assemblage and of *U. jafari* among nannofossils (Fig. 7). *N. atlantica*, a subpolar taxon (Poore and Berggren, 1975), is almost absent throughout the investigated interval, rarely reaching 1-2%, while it shows a distinct peak of abundance of ~ 10% within MIS 104. Peaks in abundance of the taxon in the Central and Eastern Mediterranean have been documented in different time intervals by several authors and specifically during MIS 116, 110, 100, 98, and 96 (Zachariasse et al., 1990; Hilgen, 1991a; Lourens et al., 1992, 1996; Becker et al., 2005; Sprovieri et al., 2006), although a correlation with Atlantic findings was not found so far. Indeed, the occurrence of the subpolar waters in mid-latitude Atlantic record based of the appearance of *N. atlantica* (Zachariasse et al., 1990; Hilgen, 1991a; Lourens et al., 1992, 1996; Becker et al., 2005; Sprovieri et al., 2006; Bolton et al., 2018) or dynoflagellate assemblage (Hennissen et al., 2015) has been documented not earlier than MIS 104, when the first southward migration of the Subarctic Front has been inferred. The older occurrences of *N. atlantica* in the Mediterranean have been related to the development of specific temperature and nutrient conditions favoring the proliferation of indigenous but previously rare populations (Bolton et al., 2018), similarly to what happened to *N. pachyderma*(s) in the late Pleistocene western Mediterranean (Rohling et al., 1998). The present documentation of *N. atlantica* during MIS 104 at MSNt-s reconciles the correlation between Atlantic and Mediterranean during MIS 104 and testifies that subpolar waters extended into the Mediterranean starting from MIS 104. The concurrent abrupt increase in the abundance of *U. jafari* (Fig. 7) supports the occurrence of marked changes in surface water conditions during MIS 104. This signal was never reported from previous studies, although the correlation of the abundance peak of the taxon with strong variations in $\delta^{18}O$

isotope record has been found elsewhere (Flores et al., 2005) and could indicate a possible increase in the evaporation/precipitation ratio and enhanced salinity (Wade and Bown, 2006; Kapid et al., 2019). It is noteworthy that this is the phase with the maximum amplitude in the precession cycle (highest value in precession maxima) (Fig. 7), likely responsible for reduced precipitation/enhanced evaporation and consequent increase in surface water salinity. We suggest that this climate framework may have favored the proliferation of *U. jafari* in the study area, sustaining the paleoenvironmental significance of the species.

The marked change recorded at MSNt-s during MIS 104 correlates with significant SST decrease in both the Mediterranean and Atlantic record (Fig. 7) and with the first increased input of silicate minerals (increase in quartz/calcite ratio in Fig. 7) as signal of ice-rafting events in the mid-latitude North Atlantic (Naafs et al., 2013). It also matches with one of the pulses of IRD discharge in northern North Atlantic as recorded at ODP Site 984 (Fig. 7), where IRD deposition became a persistent feature during glacial stages after MIS G6 (Bartoli et al., 2006), thus earlier than in the mid-latitude area. These results suggest that the evidence of the southward migration of the Subarctic Front recorded in MSNt-s is in phase with findings from the mid-latitude North Atlantic record.

The overall correlation between our oxygen isotope profile and Atlantic records (Fig. 8) further supports that $\delta^{18}O$ record of $MNS_{t\text{-}s}$ captures signals of global climate variability. In fact, in addition to the prominent climate shift recorded at MIS 104 in both Mediterranean and North Atlantic, the comparison of MSNt-s $\delta^{18}O$ record with the high-resolution planktic $\delta^{18}O$ record of IODP Site U1313, provides a finer scale correlation of several short-terms fluctuations as indicated in figure 8 by the shaded lines. This comparison highlights the occurrence of suborbital variability, mainly recorded during interglacials (Fig. 8). To this regard, the position of the Gelasian GSSP at the MSNt-s with respect to the new high resolution planktonic $\delta^{18}O$ has a special climatostratigraphic interest being located at the end of the first oxygen isotope positive shift recorded during MIS 103 (Fig. 8). This stadial phase is also well visible in the planktonic and benthic oxygen isotope Atlantic records of IODP Site U1313, thus improving the correlation potential of the GSSP outside the type-area. The good correlation of the climate fluctuations at MSNt-s with the North Atlantic planktonic isotope record (Fig. 8) highlights a connection of the Mediterranean basin with both low latitude precessional forced climate and North Atlantic climate variability during the iNHG as already well documented for Pleistocene and Holocene records (e.g. Cacho et al., 1999, 2000; Martrat et al., 2004; Sierro et al., 2005; Giaccio et al., 2015; Goñi et al., 2016; Bazzicalupo et al., 2022).

5. Conclusion

We provide the first documentation of high-resolution surface water variability in Monte San Nicola type-section, based on planktonic foraminifera stable oxygen isotopes and calcareous plankton assemblages. The acquired dataset gives clear evidence of obliquity-forced glacial-interglacial phases, extending from MIS G4 to MIS 103 (between 2.7 to 2.568 Ma), which are in phase with both Mediterranean and Atlantic reference records. Precession-related variations of thermocline/nutricline depth are also well depicted in the study section based on calcareous plankton indicating changes between deep thermocline/nutricline conditions, developing during precession minima/insolation maxima and cooler/shallower thermocline phases, established in relation with precession maxima/insolation minima. These changes are correlated with eastern Mediterranean monsoon-related African run-off proxies and reflect precessional induced wet-dry North Africa climate phases. The taxa *F. profunda, H. sellii* and *C. pelagicus* ssp. *pelagicus* among calcareous nannofossils and *G. bulloides* and *G. glutinata* within the planktonic foraminifera assemblage, were mainly affected by surface water variability on a precessional scale and suitable to capture this climate signature within the section. The heaviest $\delta^{18}O$ values, and coeval sharp increase of *N. atlantica* and of *U. jafari* recorded slightly below the GSSP location, highlight that a relevant change occurred in surface water during MIS 104. This event marks the first evidence of relationship between Mediterranean cooling event and southward migration of the Subarctic Front in the mid-latitude and give evidence of intensification of North Hemisphere Glaciation within the type-section. Finally, the overall dataset provides a precise location of the Gelasian GSSP within MIS 103, and specifically at the end of the first oxygen isotope positive shift during the interglacial, thus improving its correlation potential outside the type-area.

Acknowledgments

This research falls within the GELSTRAT Project sponsored by INQUA-SACCOM-SQS. It benefited from financial supports by PhD fellowship to M. Addante - Università degli Studi di Bari Aldo Moro, Fondi Ateneo assigned to P. Maiorano, 2018, IRIS PRJ-0686 and 2017-QUAD-0015 assigned to A. Caruso to and FFR2021/2022 G. Scopelliti. Instrumental upgrades from “Potenziamento Strutturale PONa3_00369 dell'Università degli Studi di Bari, Laboratorio per lo Sviluppo Integrato delle Scienze e delle TEcnologie dei Materiali Avanzati e per dispositivi innovativi (SISTEMA)” are also acknowledged.

References

Aitchison, J., 1986. The Statistical Analysis of Compositional Data. Springer Netherlands, Dordrecht. https://doi.org/10.1007/978-94-009-4109-0

Aitchison, J., 1981. A new approach to null correlations of proportions. Journal of the International Association for Mathematical Geology 13, 175–189. https://doi.org/10.1007/BF01031393

André, A., Weiner, A., Quillévéré, F., Aurahs, R., Morard, R., Douady, C.J., de Garidel-Thoron, T., Escarguel, G., de Vargas, C., Kucera, M., 2013. The cryptic and the apparent reversed: lack of genetic differentiation within the morphologically diverse plexus of the planktonic foraminifer "Globigerinoides sacculifer." Paleobiology 39, 21–39.

Aubry, M.-P., 1992. Paleogene Calcareous Nannofossils from the Kerguelen Plateau, Leg 120, in: Proceedings of the Ocean Drilling Program, 120 Scientific Results. Ocean Drilling Program. https://doi.org/10.2973/odp.proc.sr.120.149.1992

Aurahs, R., Treis, Y., Darling, K., Kucera, M., 2011. A revised taxonomic and phylogenetic concept for the planktonic foraminifer species Globigerinoides ruber based on molecular and morphometric evidence. Mar Micropaleontol 79, 1–14. https://doi.org/10.1016/j.marmicro.2010.12.001

Backman, J., 1984. Cenozoic Calcareous Nannofossil Biostratigraphy from the Northeastern Atlantic Ocean—Deep Sea Drilling Project Leg 81, in: Initial Reports of the Deep Sea Drilling Project, 81. U.S. Government Printing Office. https://doi.org/10.2973/dsdp.proc.81.105.1984

Bárcena, M.A., Flores, J.A., Sierro, F.J., Pérez-Folgado, M., Fabres, J., Calafat, A., Canals, M., 2004. Planktonic response to main oceanographic changes in the Alboran Sea (Western Mediterranean) as documented in sediment traps and surface sediments. Mar Micropaleontol 53, 423–445. https://doi.org/10.1016/j.marmicro.2004.09.009

Bartoli, G., Sarnthein, M., Weinelt, M., 2006. Late Pliocene millennial-scale climate variability in the northern North Atlantic prior to and after the onset of Northern Hemisphere glaciation. Paleoceanography 21. https://doi.org/10.1029/2005PA001185

Baumann, K.-H., Andruleit, H., Samtleben, C., 2000. Coccolithophores in the Nordic Seas: comparison of living communities with surface sediment assemblages. Deep Sea Research Part II: Topical Studies in Oceanography 47, 1743–1772. https://doi.org/10.1016/S0967-0645(00)00005-9

Bazzicalupo, P., Sicre, M.-A., Checa, H., Maiorano, P., Margaritelli, G., Klein, V., Pena, L.D., Cacho, I., Frigola, J., Bonomo, S., 2022. Climate evolution in the Adriatic Sea across the last deglaciation: A multiproxy approach combining biomarkers and calcareous plankton. Palaeogeogr Palaeoclimatol Palaeoecol 608, 111291.

Bé, A.W.H., 1977. An ecological, zoogeographic and taxonomic review of recent planktonic foraminifera.

Bé, A.W.H., Hamlin, W.H., 1967. Ecology of Recent Planktonic Foraminifera: Part 3: Distribution in the North Atlantic during the Summer of 1962. Micropaleontology 13, 87. https://doi.org/10.2307/1484808

Bé, A.W.H., Tolderlund, D.S., 1971. Distribution and ecology of living planktonic foraminifera in surface waters of the Atlantic and Indian Oceans. In: The micropaleontology of the Oceans. Cambridge University Press.

Bé, A.W.H., Vilks, G., Lott, L., Be, A.W.H., 1971. Winter Distribution of Planktonic Foraminifera between the Grand Banks and the Caribbean. Micropaleontology 17, 31. https://doi.org/10.2307/1485035

Bé, A.W.H., Bishop, J.K.B., Sverdlove, M.S., Gardner, W.D., 1985. Standing stock, vertical distribution and flux of planktonic foraminifera in the Panama Basin. Mar Micropaleontol 9, 307–333. https://doi.org/10.1016/0377-8398(85)90002-7

Beaufort, L., Lancelot, Y., Camberlin, P., Cayre, O., Vincent, E., Bassinot, F., Labeyrie, L., 1997. Insolation Cycles as a Major Control of Equatorial Indian Ocean Primary Production. Science (1979) 278, 1451–1454. https://doi.org/10.1126/science.278.5342.1451

Becker, J., Lourens, L.J., Hilgen, F.J., van der Laan, E., Kouwenhoven, T.J., Reichart, G.-J., 2005. Late Pliocene climate variability on Milankovitch to millennial time scales: A high-resolution study of MIS100 from the Mediterranean. Palaeogeogr Palaeoclimatol Palaeoecol 228, 338–360. https://doi.org/10.1016/j.palaeo.2005.06.020

Berggren, W.A., 1972. Cenozoic Biostratigraphy and Paleobiogeography of the North Atlantic, in: Initial Reports of the Deep Sea Drilling Project, 12. U.S. Government Printing Office. https://doi.org/10.2973/dsdp.proc.12.114.1972

Béthoux, J.P., 1993. Mediterranean sapropel formation, dynamic and climatic viewpoints. Oceanologica Acta 16, 127–133.

Boeckel, B., Baumann, K.-H., 2008. Vertical and lateral variations in coccolithophore community structure across the subtropical frontal zone in the South Atlantic Ocean. Mar Micropaleontol 67, 255–273.

Bolton, C.T., Wilson, P.A., Bailey, I., Friedrich, O., Beer, C.J., Becker, J., Baranwal, S., Schiebel, R., 2010. Millennial-scale climate variability in the subpolar North Atlantic Ocean during the late Pliocene. Paleoceanography 25, n/a-n/a. https://doi.org/10.1029/2010PA001951

Bolton, C.T., Bailey, I., Friedrich, O., Tachikawa, K., Garidel-Thoron, T., Vidal, L., Sonzogni, C., Marino, G., Rohling, E.J., Robinson, M.M., Ermini, M., Koch, M., Cooper, M.J., Wilson, P.A., 2018. North Atlantic Midlatitude Surface-Circulation Changes Through the Plio-Pleistocene Intensification of Northern Hemisphere Glaciation. Paleoceanogr Paleoclimatol 33, 1186–1205. https://doi.org/10.1029/2018PA003412

Bonfardeci, A., Caruso, A., Bartolini, A., Bassinot, F., Blanc-Valleron, M.-M., 2018. Distribution and ecology of the Globigerinoides ruber — Globigerinoides elongatus morphotypes in the Azores region during the late Pleistocene-Holocene. Palaeogeogr Palaeoclimatol Palaeoecol 491, 92–111. https://doi.org/10.1016/j.palaeo.2017.11.052

Bonomo, S., Cascella, A., Alberico, I., Ferraro, L., Giordano, L., Lirer, F., Vallefuoco, M., Marsella, E., 2014. Coccolithophores from near the Volturno estuary (central Tyrrhenian Sea). Mar. Micropaleontol. 111, 26–37. https://doi.org/10.1016/j. marmicro.2014.06.001.

Bonomo S, Schroeder K, Cascella A, Alberico I, Lirer F., 2021. Living coccolithophore communities in the central Mediterranean Sea (Summer 2016): Relations between ecology and oceanography. Mar Micropaleontol. May;165:101995.

Bosmans, J.H.C., Hilgen, F.J., Tuenter, E., Lourens, L.J., 2015. Obliquity forcing of low-latitude climate. Climate of the Past 11, 1335–1346. https://doi.org/10.5194/cp-11-1335-2015

Cacho, I., Grimalt, J.O., Pelejero, C., Canals, M., Sierro, F.J., Flores, J.A., Shackleton, N., 1999. Dansgaard-Oeschger and Heinrich event imprints in Alboran Sea paleotemperatures. Paleoceanography 14, 698–705.

Cacho, I., Grimalt, J.O., Sierro, F.J., Shackleton, N., Canals, M., 2000. Evidence for enhanced Mediterranean thermohaline circulation during rapid climatic coolings. Earth Planet Sci Lett 183, 417–429.

Capraro, L., Bonomo, S., Di Stefano, A., Ferretti, P., Fornaciari, E., Galeotti, S., Incarbona, A., Macrì, P., Raffi, I., Sabatino, N., Speranza, F., Sprovieri, M., Di Stefano, E., Sprovieri, R., Rio, D., 2022. The Monte San Nicola section (Sicily) revisited: A potential unit-stratotype of the Gelasian Stage. Quat Sci Rev 278, 107367. https://doi.org/10.1016/J.QUASCIREV.2021.107367

Caruso, A., 2004. Climatic changes during late Pliocene and early Pleistocene at Capo Rossello (Sicily, Italy): response from planktonic foraminifera. In Proceedings of the First Italian Meeting on Environmental Micropaleontology: Grzybowski Foundation Special publication .

Castradori, D., 1992. I nannofossili calcarei come strumento per lo studio biostratigrafico e paleoceanografico del Quaternario nel Mediterraneo Orientale. Unpublished Ph.D. Thesis. University of Milano,Italy.

Castradori, D., Rio, D., Hilgen, F.J., Lourens, L.J., 1998. The Global Standard Stratotype-section and Point (GSSP) of the Piacenzian Stage (Middle Pliocene). Episodes 21, 88–93. https://doi.org/10.18814/epiiugs/1998/v21i2/003

Catalano, R., Valenti, V., Albanese, C., Accaino, F., Sulli, A., Tinivella, U., Gasparo Morticelli, M., Zanolla, C., Giustiniani, M., 2013. Sicily's fold–thrust belt and slab roll-back: the SI.RI.PRO. seismic crustal transect. J Geol Soc London 170, 451–464. https://doi.org/10.1144/jgs2012-099

Channell, J., Di Stefano, E., Sprovieri, R., 1992. Calcareous plankton biostratigraphy, magnetostratigraphy and paleoclimatic history of the Plio-Pleistocene Monte San Nicola section (southern Sicily). Bollettino - Societa Paleontologica Italiana 31, 351–382.

Chepstow-Lusty, A., Backman, J., Shackleton, N.J., 1989. Comparison of upper Pliocene Discoaster abundance variations from North Atlantic Sites 552, 607, 658, 659 and 662: further evidence for marine plankton responding to orbital forcing. In Ruddiman, WF, Sarnthein, M., et al., Proc. ODP, Sci. Results.

Chepstow-Lusty, A., Backman, J., Shackleton, N.J., 1992. Comparison of Upper Pliocene Discoaster abundance variations from the Atlantic, Pacific and Indian Oceans: the significance of productivity pressure at low latitudes. Memorie di Scienze Geologiche 44, 357–373.

Cita, M.B., Gartner, S., 1973. Studi sul pliocene a sugli strati di passaggio dal miocene al pliocene. Iv. The stratotype zanclean. Foraminiferal and nannofossil biostratigraphy. Rivista Italiana Paleontologia Stratigrafica 79, 503–557.

Colmenero-Hidalgo, E., Flores, J.-A., Sierro, F.J., Bárcena, M.Á., Löwemark, L., Schönfeld, J., Grimalt, J.O., 2004. Ocean surface water response to short-term climate changes revealed by coccolithophores from the Gulf of Cadiz (NE Atlantic) and Alboran Sea (W Mediterranean). Palaeogeogr Palaeoclimatol Palaeoecol 205, 317–336. https://doi.org/10.1016/j.palaeo.2003.12.014

Corselli, C., Principato, M.S., Maffioli, P., Crudeli, D., 2002. Changes in planktonic assemblages during sapropel S5 deposition: Evidence from Urania Basin area, eastern Mediterranean. Paleoceanography 17, 1-1-1–30. https://doi.org/10.1029/2000PA000536

Darling, K.F., Kucera, M., Kroon, D., Wade, C.M., 2006. A resolution for the coiling direction paradox in *Neogloboquadrina pachyderma*. Paleoceanography 21, n/a-n/a. https://doi.org/10.1029/2005PA001189

Dowsett, H.J., Poore, R.Z., 1990. A new planktic foraminifer transfer function for estimating pliocene—Holocene paleoceanographic conditions in the North Atlantic. Mar Micropaleontol 16, 1–23. https://doi.org/10.1016/0377-8398(90)90026-I

Dowsett, H.J., Robinson, M.M., 2007. Mid-Pliocene planktic foraminifer assemblage of the North Atlantic Ocean. Micropaleontology 53, 105–126. https://doi.org/10.2113/gsmicropal.53.1-2.105

Driever, B.W.M., 1988. Calcareous nannofossil biostratigraphy and paleoenvironmental interpretation of the Mediterranean Pliocene. PhD Thesis . Utrecht University.

Emeis, K.-C., Sakamoto, T., Wehausen, R., Brumsack, H.-J., 2000a. The sapropel record of the eastern Mediterranean Sea — results of Ocean Drilling Program Leg 160. Palaeogeogr Palaeoclimatol Palaeoecol 158, 371–395. https://doi.org/10.1016/S0031-0182(00)00059-6

Emeis, K.-C., Struck, U., Schulz, H.-M., Rosenberg, R., Bernasconi, S., Erlenkeuser, H., Sakamoto, T., Martinez-Ruiz, F., 2000b. Temperature and salinity variations of Mediterranean Sea surface waters over the last 16,000 years from records of planktonic stable oxygen isotopes and alkenone unsaturation ratios. Palaeogeogr Palaeoclimatol Palaeoecol 158, 259–280. https://doi.org/10.1016/S0031-0182(00)00053-5

Emeis, K.-C., Schulz, H., Struck, U., Rossignol-Strick, M., Erlenkeuser, H., Howell, M.W., Kroon, D., Mackensen, A., Ishizuka, S., Oba, T., Sakamoto, T., Koizumi, I., 2003. Eastern Mediterranean surface water temperatures and $\delta^{18}O$ composition during deposition of sapropels in the late Quaternary. Paleoceanography 18, n/a-n/a. https://doi.org/10.1029/2000PA000617

Fairbanks, R.G., Wiebe, P.H., 1980. Foraminifera and Chlorophyll Maximum: Vertical Distribution, Seasonal Succession, and Paleoceanographic Significance. Science (1979) 209, 1524–1526. https://doi.org/10.1126/science.209.4464.1524

Fairbanks, R.G., Wiebe, P.H., Bé, A.W.H., 1980. Vertical Distribution and Isotopic Composition of Living Planktonic Foraminifera in the Western North Atlantic. Science (1979) 207, 61–63. https://doi.org/10.1126/science.207.4426.61

Farouk, S., Jain, S., Abd-Elazez, M., El Shennawy, T., Shaker, F., 2021. High-resolution Pliocene–Pleistocene calcareous nannofossil distribution and palaeoenvironmental changes in the northwest Nile Delta, Egypt. Lethaia 54, 845–870. https://doi.org/10.1111/let.12444

Flores, J.A., Sierro, F.-J., 1987. Calcareous plankton in the Tortonian/Messinian Transition Series of the northwestern edge of the Guadalquivir Basin. Abh. Geol. Bundesanst 39, 67–84.

Flores, J.A., Sierro, F.J., Glaçon, G., 1992. Calcareous plankton analysis in the pre-evaporitic sediments of the ODP Site 654 (Tyrrhenian Sea, Western Mediterranean). Micropaleontology 279–288.

Flores, J.A., Sierro, F.J., Raffi, I., 1995. Evolution of the calcareous nannofossil assemblage as a response to the paleoceanographic changes in the eastern equatorial Pacific Ocean from 4 to 2 Ma (Leg 138, Sites 849 and 852) . Proceedings of the Ocean Drilling Program, Scientific Results 138, 163–176.

Flores, J.A., Sierro, F.J., 1997. Revised technique for calculation of calcareous nannofossil accumulation rates. Micropaleontology 321–324.

Flores, J.A., Bárcena, M.A., Sierro, F.J., 2000. Ocean-surface and wind dynamics in the Atlantic Ocean off Northwest Africa during the last 140 000 years. Palaeogeogr Palaeoclimatol Palaeoecol 161, 459–478. https://doi.org/10.1016/S0031-0182(00)00099-7

Flores, J.A., Sierro, F.J., Filippelli, G.M., Bárcena, M.Á., Pérez-Folgado, M., Vázquez, A., Utrilla, R., 2005. Surface water dynamics and phytoplankton communities during deposition of cyclic late Messinian sapropel sequences in the western Mediterranean. Mar Micropaleontol 56, 50–79. https://doi.org/10.1016/j.marmicro.2005.04.002

Gasparo Morticelli, M., Valenti, V., Catalano, R., Sulli, A., Agate, M., Avellone, G., Albanese, C., Basilone, L., Gugliotta, C., 2015. Deep controls on foreland basin system evolution along the Sicilian fold and thrust belt. Bulletin de la Société Géologique de France 186, 273–290. https://doi.org/10.2113/gssgfbull.186.4-5.273

Geisen, M., Billard, C., Broerse, A., Cros, L., Probert, I., Young, J., 2002. Life-cycle associations involving pairs of holococcolithophorid species: intraspecific variation or cryptic speciation? Eur J Phycol 37, 531–550. https://doi.org/10.1017/S0967026202003852

Geraga, M., Tsaila-Monopolis, S., Ioakim, C., Papatheodorou, G., Ferentinos, G., 2005. Short-term climate changes in the southern Aegean Sea over the last 48,000 years. Palaeogeogr Palaeoclimatol Palaeoecol 220, 311–332. https://doi.org/10.1016/j.palaeo.2005.01.010

Geraga, M., Mylona, G., Tsaila-Monopoli, St., Papatheodorou, G., Ferentinos, G., 2008. Northeastern Ionian Sea: Palaeoceanographic variability over the last 22 ka. Journal of Marine Systems 74, 623–638. https://doi.org/10.1016/j.jmarsys.2008.05.019

Geraga, M., Ioakim, Chr., Lykousis, V., Tsaila-Monopolis, S., Mylona, G., 2010. The high-resolution palaeoclimatic and palaeoceanographic history of the last 24,000years in the central Aegean Sea, Greece. Palaeogeogr Palaeoclimatol Palaeoecol 287, 101–115. https://doi.org/10.1016/j.palaeo.2010.01.023

Giaccio, B., Regattieri, E., Zanchetta, G., Nomade, S., Renne, P.R., Sprain, C.J., Drysdale, R.N., Tzedakis, P.C., Messina, P., Scardia, G., 2015. Duration and dynamics of the best orbital analogue to the present interglacial. Geology 43, 603–606.

Gibbard, P.L., Head, M.J., 2010. The newly-ratified definition of the Quaternary System/Period and redefinition of the Pleistocene Series/Epoch, and comparison of proposals advanced prior to formal ratification. Episodes 33, 152–158. https://doi.org/10.18814/epiiugs/2010/v33i3/002

Gibbard, P.L., Head, M.J., Walker, M.J.C., 2010. Formal ratification of the Quaternary System/Period and the Pleistocene Series/Epoch with a base at 2.58 Ma. J Quat Sci 25, 96–102. https://doi.org/10.1002/jqs.1338

Gibbs, S., Shackleton, N., Young, J., 2004. Orbitally forced climate signals in mid-Pliocene nannofossil assemblages. Mar Micropaleontol 51, 39–56. https://doi.org/10.1016/j.marmicro.2003.09.002

Goñi, M.F.S., Rodrigues, T., Hodell, D.A., Polanco-Martinez, J.M., Alonso-Garcia, M., Hernandez-Almeida, I., Desprat, S., Ferretti, P., 2016. Tropically-driven climate shifts in southwestern Europe during MIS 19, a low eccentricity interglacial. Earth Planet Sci Lett 448, 81–93.

Grant, K.M., Grimm, R., Mikolajewicz, U., Marino, G., Ziegler, M., Rohling, E.J., 2016. The timing of Mediterranean sapropel deposition relative to insolation, sea-level and African monsoon changes. Quat Sci Rev 140, 125–141. https://doi.org/10.1016/j.quascirev.2016.03.026

Grant, K.M., Rohling, E.J., Westerhold, T., Zabel, M., Heslop, D., Konijnendijk, T., Lourens, L., 2017. A 3 million year index for North African humidity/aridity and the implication of potential pan-African Humid periods. Quat Sci Rev 171, 100–118. https://doi.org/10.1016/j.quascirev.2017.07.005

Grant, K.M., Amarathunga, U., Amies, J.D., Hu, P., Qian, Y., Penny, T., Rodriguez-Sanz, L., Zhao, X., Heslop, D., Liebrand, D., Hennekam, R., Westerhold, T., Gilmore, S., Lourens, L.J., Roberts, A.P., Rohling, E.J., 2022. Organic carbon burial in Mediterranean sapropels intensified during Green Sahara Periods since 3.2 Myr ago. Commun Earth Environ 3, 11. https://doi.org/10.1038/s43247-021-00339-9

Grelaud, M., Marino, G., Ziveri, P., Rohling, E.J., 2012. Abrupt shoaling of the nutricline in response to massive freshwater flooding at the onset of the last interglacial sapropel event. Paleoceanography 27, n/a-n/a. https://doi.org/10.1029/2012PA002288

Haidar, A.T., Thierstein, H.R., 2001. Coccolithophore dynamics off Bermuda (N. Atlantic). Deep Sea Res 2 Top Stud Oceanogr 48, 1925–1956. https://doi.org/10.1016/S0967-0645(00)00169-7

Hammer, Ø., Harper, D.A., 2001. Past: paleontological statistics software package for educaton and data anlysis. Palaeontologia electronica 4.

Haq, B.U., 1980. Biogeographic history of Miocene calcareous nannoplankton and paleoceanography of the Atlantic Ocean. Micropaleontology 414–443.

Head, M.J., 2019. Formal subdivision of the Quaternary System/Period: Present status and future directions. Quaternary International 500, 32–51.

Hemleben, C., Spindler, M., Anderson, O.R., 1989. Modern Planktonic Foraminifera. Springer New York, New York, NY. https://doi.org/10.1007/978-1-4612-3544-6

Hennekam, R., Jilbert, T., Schnetger, B., De Lange, G.J., 2014. Solar forcing of Nile discharge and sapropel S1 formation in the early to middle Holocene eastern Mediterranean. Paleoceanography 29, 343–356. https://doi.org/10.1002/2013PA002553

Hennekam, R., Donders, T.H., Zwiep, K., de Lange, G.J., 2015. Integral view of Holocene precipitation and vegetation changes in the Nile catchment area as inferred from its delta sediments. Quat Sci Rev 130, 189–199. https://doi.org/10.1016/j.quascirev.2015.05.031

Hennissen, J.A.I., Head, M.J., De Schepper, S., Groeneveld, J., 2014. Palynological evidence for a southward shift of the North Atlantic Current at ~2.6 Ma during the intensification of late Cenozoic Northern Hemisphere glaciation. Paleoceanography 29, 564–580. https://doi.org/10.1002/2013PA002543

Hennissen, J.A.I., Head, M.J., De Schepper, S., Groeneveld, J., 2015. Increased seasonality during the intensification of Northern Hemisphere glaciation at the Pliocene–Pleistocene boundary ~2.6 Ma. Quat Sci Rev 129, 321–332. https://doi.org/10.1016/j.quascirev.2015.10.010

Herbert, T.D., Ng, G., Cleaveland Peterson, L., 2015. Evolution of Mediterranean sea surface temperatures 3.5–1.5 Ma: Regional and hemispheric influences. Earth Planet Sci Lett 409, 307–318. https://doi.org/10.1016/j.epsl.2014.10.006

Herbert, T.D., Lawrence, K.T., Tzanova, A., Peterson, L.C., Caballero-Gill, R.P., Kelly, C.S., 2018. (Table S2) SST esimates as a function of age, Mediterranean sites. PANGAEA. https://doi.org/10.1594/PANGAEA.885603

Hilgen, F.J., 1991a. Astronomical calibration of Gauss to Matuyama sapropels in the Mediterranean and implication for the Geomagnetic Polarity Time Scale. Earth Planet Sci Lett 104, 226–244. https://doi.org/10.1016/0012-821X(91)90206-W

Hilgen, F.J., 1991b. Extension of the astronomically calibrated (polarity) time scale to the Miocene/Pliocene boundary. Earth Planet Sci Lett 107, 349–368. https://doi.org/10.1016/0012-821X(91)90082-S

Hilgen, Krijgsman, 1999. Cyclostratigraphy and astrochronology of the Tripoli diatomite formation (pre-evaporite Messinian, Sicily, Italy). Terra Nova 11, 16–22. https://doi.org/https://doi.org/10.1046/j.1365-3121.1999.00221.x

Howell, M.W., Thunell, R.C., Di Stefano, E., Sprovieri, R., Tappa, E.J., Sakamoto, T., 1998. Stable isotope chronology and paleoceanographic history of sites 963 and 964, eastern mediterranean sea, in: Robertson, A.H.F., Emeis, K.C., Richter, C., Camerlenghi, A. (Eds.), Proceedings of the Ocean Drilling Program, Scientific Results. .

Incarbona, A., Di Stefano, E., 2019. Calcareous nannofossil palaeoenvironmental reconstruction and preservation in sapropel S1 at the Eratosthenes Seamount (Eastern Mediterranean). Deep Sea Res 2 Top Stud Oceanogr 164, 206–215. https://doi.org/10.1016/j.dsr2.2018.10.004

Incarbona, A., Ziveri, P., Sabatino, N., Manta, D.S., Sprovieri, M., 2011. Conflicting coccolithophore and geochemical evidence for productivity levels in the Eastern Mediterranean sapropel S1. Mar Micropaleontol 81, 131–143. https://doi.org/10.1016/j.marmicro.2011.09.003

Jenkins, J.A., Williams, D.F., 1984. Nile water as a cause of eastern Mediterranean sapropel formation: evidence for and against. Mar Micropaleontol 8, 521–534.

Jilbert, T., Reichart, G.-J., Mason, P., De Lange, G.J., 2010. Short-time-scale variability in ventilation and export productivity during the formation of Mediterranean sapropel S1. Paleoceanography 25. https://doi.org/10.1029/2010PA001955

Jordan, W.R., Cros, L., Young, R.J., 2004. A Revised Classification Scheme for Living Haptophytes. Micropaleontology 50, 55–79.

Kallel, N., Duplessy, J.-C., Labeyrie, L., Fontugne, M., Paterne, M., Montacer, M., 2000. Mediterranean pluvial periods and sapropel formation over the last 200 000 years. Palaeogeogr Palaeoclimatol Palaeoecol 157, 45–58. https://doi.org/10.1016/S0031-0182(99)00149-2

Kapid, R., Santoso, W.D., Ikhsan, B., Jambak, M.A., Irawan, D.E., 2019. The Mid Miocene Climatic Optimum (MMCO) Indication at Low Latitude Sediment Case Study: The Miocene Cibulakan Formation, Bogor Basin, Indonesia. Int J Adv Sci Eng Inf Technol 9, 594. https://doi.org/10.18517/ijaseit.9.2.7573

Kemp, A.E.S., Pearce, R.B., Koizumi, I., Pike, J., Rance, S.J., 1999. The role of mat-forming diatoms in the formation of Mediterranean sapropels. Nature 398, 57–61. https://doi.org/10.1038/18001

Kleijne, A., 1993. Morphology, taxonomy and distribution of extant coccolithophorids (calcareous nannoplankton). Drukkerij FEBO BV.

Kleiven, H.F., Jansen, E., Fronval, T., Smith, T.M., 2002. Intensification of Northern Hemisphere glaciations in the circum Atlantic region (3.5–2.4 Ma)–ice-rafted detritus evidence. Palaeogeogr Palaeoclimatol Palaeoecol 184, 213–223.

Konijnendijk, T.Y.M., Ziegler, M., Lourens, L.J., 2014. Chronological constraints on Pleistocene sapropel depositions from high-resolution geochemical records of ODP Sites 967 and 968. Newsl Stratigr 47, 263–282. https://doi.org/10.1127/0078-0421/2014/0047

Laskar, J., Robutel, P., Joutel, F., Gastineau, M., Correia, A.C.M., Levrard, B., 2004. A long-term numerical solution for the insolation quantities of the Earth. Astron Astrophys 428, 261–285. https://doi.org/10.1051/0004-6361:20041335

Lentini, F., Carbone, S., 2014. Geologia della Sicilia-ISPRA. Memorie Descrittive della Carta Geologica d'Italia.

Lirer, F., Foresi, L.M., Iaccarino, S.M., Salvatorini, G., Turco, E., Cosentino, C., Sierro, F.J., Caruso, A., 2019. Mediterranean Neogene planktonic foraminifer biozonation and biochronology. Earth Sci Rev 196, 102869.

Lisiecki, L.E., Raymo, M.E., 2005. A Pliocene-Pleistocene stack of 57 globally distributed benthic δ^{18}O records. Paleoceanography 20, n/a-n/a. https://doi.org/10.1029/2004PA001071

Lohmann, G.P., Carlson, J.J., 1981. Oceanographic significance of Pacific late miocene calcareous nannoplankton. Mar Micropaleontol 6, 553–579. https://doi.org/10.1016/0377-8398(81)90021-9

Loubere, P., Moss, K., 1986. Late Pliocene climatic change and the onset of Northern Hemisphere glaciation as recorded in the northeast Atlantic Ocean. GSA Bulletin 97, 818–828. https://doi.org/10.1130/0016-7606(1986)97<818:LPCCAT>2.0.CO;2

Lourens, L.J., Hilgen, F.J., Gudjonsson, L., Zachariasse, W.J., 1992. Late Pliocene to early Pleistocene astronomically forced sea surface productivity and temperature variations in the Mediterranean. Mar Micropaleontol 19, 49–78. https://doi.org/10.1016/0377-8398(92)90021-B

Lourens, L.J., Antonarakou, A., Hilgen, F.J., Van Hoof, A.A.M., Vergnaud-Grazzini, C., Zachariasse, W.J., 1996. Evaluation of the Plio-Pleistocene astronomical timescale. Paleoceanography 11, 391–413.

Lourens, L.J., Hilgen, F.J., Raffi, I., 1998. Base of large Gephyrocapsa and astronomical calibration of early Pleistocene sapropels in Site 967 and Hole 969D: solving the chronology of the Vrica section (Calabria, Italy), in: Proceeding of the Ocean Drilling Program, Scientific Results. pp. 191–197.

Lourens, L.J., Wehausen, R., Brumsack, H.J., 2001. Geological constraints on tidal dissipation and dynamical ellipticity of the Earth over the past three million years. Nature 409, 1029–1033. https://doi.org/10.1038/35059062

Maiorano, P., Tarantino, F., Marino, M., De Lange, G.J., 2013. Paleoenvironmental conditions at Core KC01B (Ionian Sea) through MIS 13–9: Evidence from calcareous nannofossil assemblages. Quaternary International 288, 97–111. https://doi.org/10.1016/j.quaint.2011.12.007

Maiorano, P., Girone, A., Marino, M., Kucera, M., Pelosi, N., 2016. Sea surface water variability during the Mid-Brunhes inferred from calcareous plankton in the western Mediterranean (ODP Site 975). Palaeogeogr Palaeoclimatol Palaeoecol 459, 229–248. https://doi.org/10.1016/j.palaeo.2016.07.006

Maiorano, P., Marino, M., De Lange, G.J., 2019. Dynamic surface-water alterations during sapropel S1 preserved in high-resolution shallow-water sediments of Taranto Gulf, central Mediterranean. Palaeogeogr Palaeoclimatol Palaeoecol 534, 109340. https://doi.org/10.1016/j.palaeo.2019.109340

Maiorano, P., Herbert, T. D., Marino, M., Bassinot, F., Bazzicalupo, P., Bertini, A., Girone, A., Nomade, S., Ciaranfi, N., 2021. Paleoproductivity modes in central Mediterranean during MIS 20—MIS 18: Calcareous plankton and alkenone variability. Paleoceanography and Paleoclimatology, 36, e2021PA004259. https://doi. org/10.1029/2021PA004259

Marino, G., Rohling, E.J., Sangiorgi, F., Hayes, A., Casford, J.L., Lotter, A.F., Kucera, M., Brinkhuis, H., 2009. Early and middle Holocene in the Aegean Sea: interplay between high and low latitude climate variability. Quat Sci Rev 28, 3246–3262.

Marino, M., Girone, A., Maiorano, P., Di Renzo, R., Piscitelli, A., Flores, J.-A., 2018. Calcareous plankton and the mid-Brunhes climate variability in the Alboran Sea (ODP Site 977). Palaeogeogr Palaeoclimatol Palaeoecol 508, 91–106. https://doi.org/10.1016/j.palaeo.2018.07.023

Martrat, B., Grimalt, J.O., Lopez-Martinez, C., Cacho, I., Sierro, F.J., Flores, J.A., Zahn, R., Canals, M., Curtis, J.H., Hodell, D.A., 2004. Abrupt temperature changes in the Western Mediterranean over the past 250,000 years. Science (1979) 306, 1762–1765.

Maslin, M.A., Li, X.S., Loutre, M.-F., Berger, A., 1998. The contribution of orbital forcing to the progressive intensification of Northern Hemisphere glaciation. Quat Sci Rev 17, 411–426.

McClymont, E.L., Ho, S.L., Ford, H.L., Bailey, I., Berke, M.A., Bolton, C.T., De Schepper, S., Grant, G.R., Groeneveld, J., Inglis, G.N., Karas, C., Patterson, M.O., Swann, G.E.A., Thirumalai, K., White, S.M., Alonso-Garcia, M., Anand, P., Hoogakker, B.A.A., Littler, K., Petrick, B.F., Risebrobakken, B., Abell, J.T., Crocker, A.J., de Graaf, F., Feakins, S.J., Hargreaves, J.C., Jones, C.L., Markowska, M., Ratnayake, A.S., Stepanek, C., Tangunan, D., 2023. Climate Evolution Through the Onset and Intensification of Northern Hemisphere Glaciation. Reviews of Geophysics 61. https://doi.org/10.1029/2022RG000793

McIntyre, A., Bé, A.W.H., 1967. Modern coccolithophoridae of the atlantic ocean—I. Placoliths and cyrtoliths. Deep Sea Research and Oceanographic Abstracts 14, 561–597. https://doi.org/10.1016/0011-7471(67)90065-4

Molfino, B., McIntyre, A., 1990. Precessional Forcing of Nutricline Dynamics in the Equatorial Atlantic. Science (1979) 249, 766–769. https://doi.org/10.1126/science.249.4970.766

Mudelsee, M., Raymo, M.E., 2005. Slow dynamics of the Northern Hemisphere glaciation. Paleoceanography 20, n/a-n/a. https://doi.org/10.1029/2005PA001153

Mulitza, S., Bickert, T., Bostock, H.C., Chiessi, C.M., Donner, B., Govin, A., Harada, N., Huang, E., Johnstone, H., Kuhnert, H., Langner, M., Lamy, F., Lembke-Jene, L., Lisiecki, L., Lynch-Stieglitz, J., Max, L., Mohtadi, M., Mollenhauer, G., Muglia, J., Nürnberg, D., Paul, A., Rühlemann, C., Repschläger, J., Saraswat, R., Schmittner, A., Sikes, E.L., Spielhagen, R.F., Tiedemann, R., 2022. World Atlas of late Quaternary Foraminiferal Oxygen and Carbon Isotope Ratios. Earth Syst Sci Data 14, 2553–2611. https://doi.org/10.5194/essd-14-2553-2022

Munz, P.M., Siccha, M., Lückge, A., Böll, A., Kucera, M., Schulz, H., 2015. Decadal-resolution record of winter monsoon intensity over the last two millennia from planktic foraminiferal assemblages in the northeastern Arabian Sea. Holocene 25, 1756–1771. https://doi.org/10.1177/0959683615591357

Naafs, B.D.A., Hefter, J., Acton, G., Haug, G.H., Martínez-Garcia, A., Pancost, R., Stein, R., 2012. Strengthening of North American dust sources during the late Pliocene (2.7 Ma). Earth Planet Sci Lett 317–318, 8–19. https://doi.org/10.1016/j.epsl.2011.11.026

Naafs, B.D.A., Hefter, J., Stein, R., 2013. Millennial-scale ice rafting events and Hudson Strait Heinrich(-like) Events during the late Pliocene and Pleistocene: a review. Quat Sci Rev 80, 1–28. https://doi.org/10.1016/j.quascirev.2013.08.014

Naidu, P.D., Malmgren, B.A., 1996. A High-resolution record of Late Quaternary upwelling along the Oman Margin, Arabian Sea based on planktonic foraminifera. Paleoceanography 11, 129–140. https://doi.org/10.1029/95PA03198

Negri, A., Capotondi, L., Keller, J., 1999. Calcareous nannofossils, planktonic foraminifera and oxygen isotopes in the late Quaternary sapropels of the Ionian Sea. Mar Geol 157, 89–103. https://doi.org/10.1016/S0025-3227(98)00135-2

Negri, A., Giunta, S., 2001. Calcareous nannofossil paleoecology in the sapropel S1 of the eastern Ionian sea: paleoceanographic implications. Palaeogeogr Palaeoclimatol Palaeoecol 169, 101–112. https://doi.org/10.1016/S0031-0182(01)00219-X

Ogniben, L., 1969. Schema introduttivo alla geologia del confine calabro-lucano. Mem. Soc. Geol. It. 8, 453–763.

Okada, H., Honjo, S., 1973. The distribution of oceanic coccolithophorids in the Pacific. Deep Sea Research and Oceanographic Abstracts 20, 355–374. https://doi.org/10.1016/0011-7471(73)90059-4

Okada, H., Wells, P., 1997. Late Quaternary nannofossil indicators of climate change in two deep-sea cores associated with the Leeuwin Current off Western Australia. Palaeogeogr Palaeoclimatol Palaeoecol 131, 413–432. https://doi.org/10.1016/S0031-0182(97)00014-X

Pinter, P.R., Butler, R.W.H., Hartley, A.J., Maniscalco, R., Baldassini, N., Di Stefano, A., 2016. The Numidian of Sicily revisited: a thrust-influenced confined turbidite system. Mar Pet Geol 78, 291–311. https://doi.org/10.1016/j.marpetgeo.2016.09.014

Pinter, P.R., Butler, R.W.H., Hartley, A.J., Maniscalco, R., Baldassini, N., Di Stefano, A., 2018. Tracking sand-fairways through a deformed turbidite system: the Numidian (Miocene) of Central Sicily, Italy. Basin Research 30, 480–501. https://doi.org/10.1111/bre.12261

Poore, R.Z., Berggren, W.A., 1975. The morphology and classification of Neogloboquadrina atlantica (Berggren). The Journal of Foraminiferal Research 5, 76–84. https://doi.org/10.2113/gsjfr.5.2.76

Pujol, C., Grazzini, C.V., 1995. Distribution patterns of live planktic foraminifers as related to regional hydrography and productive systems of the Mediterranean Sea. Mar Micropaleontol 25, 187–217. https://doi.org/10.1016/0377-8398(95)00002-I

Quintana Krupinski, N.B., Russell, A.D., Pak, D.K., Paytan, A., 2017. Core-top calibration of B/Ca in Pacific Ocean Neogloboquadrina incompta and Globigerina bulloides as a surface water carbonate system proxy. Earth Planet Sci Lett 466, 139–151. https://doi.org/10.1016/j.epsl.2017.03.007

Radmacher, W., Lempart-Drozd, M., Mikolajczak, M., Uchman, A., Head, M.J., 2023. Environmental forcing across the Neogene-Quaternary boundary at the Monte San Nicola GSSP,Sicily,Italy-preliminary results, in: XXI INQUA Conference Rome.

Raffi, I., Rio, D., 1981. Coccolithus pelagicus (Wallich): a paleotemperature indicator in the late Pliocene Mediterranean deep sea record, in: Consiglio Nazionale Delle Ricerche. International Conference. pp. 187–190.

Raymo, M.E., Ruddiman, W.F., Backman, J., Clement, B.M., Martinson, D.G., 1989. Late Pliocene variation in northern hemisphere ice sheets and North Atlantic deep water circulation. Paleoceanography 4, 413–446. https://doi.org/10.1029/PA004i004p00413

Renaud, S., Ziveri, P., Broerse, A.T.C., 2002. Geographical and seasonal differences in morphology and dynamics of the coccolithophore Calcidiscus leptoporus. Mar Micropaleontol 46, 363–385. https://doi.org/10.1016/S0377-8398(02)00081-6

Rio, D., Raffi, I., Villa, G., Kastens, K.A., 1990. Pliocene-Pleistocene calcareous nannofossil distribution patterns in the Western Mediterranean, in: Proceedings of the Ocean Drilling Program, Scientific Results. Ocean Drilling Program College Station, Texas, USA, pp. 513–533.

Rio, D., Sprovieri, R., Di Stefano, E., 1994. The Gelasian Stage: a proposal of a new chronostratigraphic unit of the Pliocene series. Revista Italiana di Palaeontologia e Stratigrafia 100, 103–124.

Rio, D., Sprovieri, R., Castradori, D., Stefano, E. Di, 1998. The Gelasian Stage (Upper Pliocene): A new unit of the global standard chronostratigraphic scale. Episodes 21, 82–87. https://doi.org/10.18814/epiiugs/1998/v21i2/002

Rohling, E.J., 1994. Review and new aspects concerning the formation of eastern Mediterranean sapropels. Mar Geol 122, 1–28. https://doi.org/10.1016/0025-3227(94)90202-X

Rohling, E.J., Gieskes, W.W.C., 1989. Late Quaternary changes in Mediterranean intermediate water density and formation rate. Paleoceanography 4, 531–545. https://doi.org/10.1029/PA004i005p00531

Rohling, E.J., Hilgen, F.J., 1991. The eastern Mediterranean climate at times of sapropel formation: a review. Geologie en Mijnbouw 70, 253–264.

Rohling, E.J., Pälike, H., 2005. Centennial-scale climate cooling with a sudden cold event around 8,200 years ago. Nature 434, 975–979. https://doi.org/10.1038/nature03421

Rohling, E.J., Jorissen, F.J., De Stigter, H.C., 1997. 200 Year interruption of Holocene sapropel formation in the Adriatic Sea. J Micropalaeontol 16, 97–108. https://doi.org/10.1144/jm.16.2.97

Rohling, E.J., Fenton, M., Jorissen, F.J., Bertrand, P., Ganssen, G., Caulet, J.P., 1998. Magnitudes of sea-level lowstands of the past 500,000 years. Nature 394, 162–165. https://doi.org/10.1038/28134

Rohling, E., Mayewski, P., Abu-Zied, R., Casford, J., Hayes, A., 2002. Holocene atmosphere-ocean interactions: records from Greenland and the Aegean Sea. Clim Dyn 18, 587–593. https://doi.org/10.1007/s00382-001-0194-8

Rossignol-Strick, M., Nesteroff, W., Olive, P., Vergnaud-Grazzini, C., 1982. After the deluge: Mediterranean stagnation and sapropel formation. Nature 295, 105–110. https://doi.org/10.1038/295105a0

Sato, T., Yuguchi, S., Takayama, T., Kameo, K., 2004. Drastic change in the geographical distribution of the cold-water nannofossil Coccolithus pelagicus (Wallich) Schiller at 2.74 Ma in the late Pliocene, with special reference to glaciation in the Arctic Ocean. Mar Micropaleontol 52, 181–193.

Schmuker, B., Schiebel, R., 2002. Planktic foraminifers and hydrography of the eastern and northern Caribbean Sea. Mar Micropaleontol 46, 387–403. https://doi.org/10.1016/S0377-8398(02)00082-8

Schulz, M., Statteger, K., 1997. SPECTRUM: A PC-program for spectral analysis of unevenly spaced time series. INQUA Sub-Commission on Data-Handling Methods Newsletter 16, 3–4.

Shackleton, N.J., Backman, J., Zimmerman, H., Kent, D. V., Hall, M.A., Roberts, D.G., Schnitker, D., Baldauf, J.G., Desprairies, A., Homrighausen, R., Huddlestun, P., Keene, J.B., Kaltenback, A.J., Krumsiek, K.A.O., Morton, A.C., Murray, J.W., Westberg-Smith, J., 1984. Oxygen isotope calibration of the onset of ice-rafting and history of glaciation in the North Atlantic region. Nature 307, 620–623. https://doi.org/10.1038/307620a0

Shackleton, N.J., Hall, M.A., Pate, D., 1995. Pliocene stable isotope stratigraphy of Site 846, in: Proc. Ocean Drill. Program Sci. Results. pp. 337–355.

Sierro, F.J., Hodell, D.A., Curtis, J.H., Flores, J.A., Reguera, I., Colmenero-Hidalgo, E., Bárcena, M.A., Grimalt, J.O., Cacho, I., Frigola, J., 2005. Impact of iceberg melting on Mediterranean thermohaline circulation during Heinrich events. Paleoceanography 20.

Silva, A., Palma, S., Moita, M.T., 2008. Coccolithophores in the upwelling waters of Portugal: Four years of weekly distribution in Lisbon bay. Cont Shelf Res 28, 2601–2613. https://doi.org/10.1016/j.csr.2008.07.009

Silva, A., Palma, S., Oliveira, P.B., Moita, M.T., 2009. Composition and interannual variability of phytoplankton in a coastal upwelling region (Lisbon Bay, Portugal). J Sea Res 62, 238–249. https://doi.org/10.1016/j.seares.2009.05.001

Silva, A., Brotas, V., Valente, A., Sá, C., Diniz, T., Patarra, R.F., Álvaro, N.V., Neto, A.I., 2013. Coccolithophore species as indicators of surface oceanographic conditions in the vicinity of Azores islands. Estuar Coast Shelf Sci 118, 50–59. https://doi.org/10.1016/j.ecss.2012.12.010

Spaak, P., 1983. Accuracy in Correlation and Ecological Aspects of the Planktonic Foraminiferal Zonation of the Mediterranean Pliocene: IGCP Project No. 1. PhD Thesis.

Spezzaferri, S., Kucera, M., Pearson, P.N., Wade, B.S., Rappo, S., Poole, C.R., Morard, R., Stalder, C., 2015. Fossil and Genetic Evidence for the Polyphyletic Nature of the Planktonic Foraminifera "Globigerinoides", and Description of the New Genus Trilobatus. PLoS One 10, e0128108. https://doi.org/10.1371/journal.pone.0128108

Sprovieri, R., 1992. Mediterranean Pliocene biochronology: an high resolution record based on quantitative planktonic foraminifera distribution. Rivista Italiana di Paleontologia e Stratigrafia 98, 61–100.

Sprovieri, R., 1993. Pliocene-early Pleistocene astronomically forced planktonic foraminifera abundance fluctuations and chronology of Mediterranean calcareous plankton bio-events. Rivista Italiana di Paleontologia e Stratigrafia 99, 371–414.

Sprovieri, R., Di Stefano, E., Incarbona, A., Oppo, D.W., 2006. Suborbital climate variability during Marine Isotopic Stage 5 in the central Mediterranean basin: evidence from calcareous plankton record. Quat Sci Rev 25, 2332–2342. https://doi.org/10.1016/j.quascirev.2006.01.035

Tangunan, D.N., Baumann, K.-H., Just, J., LeVay, L.J., Barker, S., Brentegani, L., De Vleeschouwer, D., Hall, I.R., Hemming, S., Norris, R., 2018. The last 1 million years of the extinct genus Discoaster: Plio–Pleistocene environment and productivity at Site U1476 (Mozambique Channel). Palaeogeogr Palaeoclimatol Palaeoecol 505, 187–197. https://doi.org/10.1016/j.palaeo.2018.05.043

Thomson, J., Crudeli, D., de Lange, G.J., Slomp, C.P., Erba, E., Corselli, C., Calvert, S.E., 2004. *Florisphaera profunda* and the origin and diagenesis of carbonate phases in eastern Mediterranean sapropel units. Paleoceanography 19, n/a-n/a. https://doi.org/10.1029/2003PA000976

Thunell, R.C., Reynolds, L.A., 1984. Sedimentation of Planktonic Foraminifera: Seasonal Changes in Species Flux in the Panama Basin. Micropaleontology 30, 243. https://doi.org/10.2307/1485688

Tiedemann, R., Sarnthein, M., Shackleton, N.J., 1994. Astronomic timescale for the Pliocene Atlantic δ^{18}O and dust flux records of Ocean Drilling Program Site 659. Paleoceanography 9, 619–638. https://doi.org/10.1029/94PA00208

Tolderlund, D.S., Bé, A.W.H., 1971. Seasonal Distribution of Planktonic Foraminifera in the Western North Atlantic. Micropaleontology 17, 297. https://doi.org/10.2307/1485143

Triantaphyllou, M.V., Drinia, H., Dermitzakis, M.D., 1999. Biostratigraphical and paleoenvironmental determination of a marine Plio/Pleistocene outcrop in Cefallinia Island (Greece). Géologie Méditerranéenne 26, 3–18. https://doi.org/10.3406/geolm.1999.1642

Triantaphyllou, M.V., Antonarakou, A., Dimiza, M., Anagnostou, C., 2010. Calcareous nannofossil and planktonic foraminiferal distributional patterns during deposition of sapropels S6, S5 and S1 in the Libyan Sea (Eastern Mediterranean). Geo-Marine Letters 30, 1–13. https://doi.org/10.1007/s00367-009-0145-7

Trotta, S., Marino, M., Voelker, A.H.L., Rodrigues, T., Maiorano, P., Flores, J.-A., Girone, A., Addante, M., Balestra, B., 2022. Early Pleistocene calcareous nannofossil assemblages from the Gulf of Cadiz reveal glacial-interglacial and millennial-scale variability. Palaeogeogr Palaeoclimatol Palaeoecol 608, 111304. https://doi.org/10.1016/j.palaeo.2022.111304

Vázquez, A., Utrilla, R., Zamarreño, I., Sierro, F.J., Flores, J.A., Francés, G., Bárcena, M.A., 2000. Precession-related sapropelites of the Messinian Sorbas Basin (South Spain): paleoenvironmental significance. Palaeogeogr Palaeoclimatol Palaeoecol 158, 353–370. https://doi.org/10.1016/S0031-0182(00)00058-4

Verhallen, P.M., 1987. Early development of Bulimina marginata in relation to paleoenvironmental changes in the Mediterranean. Proceedings of the Koninklijke nederlandse akademie van wetenschappen. Series B. Palaeontology, geology, physics, chemistry, anthropology 90, 160–180.

Wade, B.S., Bown, P.R., 2006. Calcareous nannofossils in extreme environments: The Messinian Salinity Crisis, Polemi Basin, Cyprus. Palaeogeogr Palaeoclimatol Palaeoecol 233, 271–286. https://doi.org/10.1016/j.palaeo.2005.10.007

Wang, L., 2000. Isotopic signals in two morphotypes of Globigerinoides ruber (white) from the South China Sea: implications for monsoon climate change during the last glacial cycle. Palaeogeogr Palaeoclimatol Palaeoecol 161, 381–394. https://doi.org/10.1016/S0031-0182(00)00094-8

Watkins, J.M., Mix, A.C., 1998. Testing the effects of tropical temperature, productivity, and mixed-layer depth on foraminiferal transfer functions. Paleoceanography 13, 96–105. https://doi.org/10.1029/97PA02904

Watkins, J.M., Mix, A.C., Wilson, J., 1996. Living planktic foraminifera: tracers of circulation and productivity regimes in the central equatorial Pacific. Deep Sea Research Part II: Topical Studies in Oceanography 43, 1257–1282. https://doi.org/10.1016/0967-0645(96)00008-2

Weaver, P.P.E., Pujol, C., 1988. History of the last deglaciation in the alboran sea (western Mediterranean) and adjacent north Atlantic as revealed by coccolith floras. Palaeogeogr Palaeoclimatol Palaeoecol 64, 35–42. https://doi.org/10.1016/0031-0182(88)90140-X

Weldeab, S., Menke, V., Schmiedl, G., 2014. The pace of East African monsoon evolution during the Holocene. Geophys Res Lett 41, 1724–1732. https://doi.org/10.1002/2014GL059361

Westerhold, T., Marwan, N., Drury, A.J., Liebrand, D., Agnini, C., Anagnostou, E., Barnet, J.S.K., Bohaty, S.M., De Vleeschouwer, D., Florindo, F., Frederichs, T., Hodell, D.A., Holbourn, A.E., Kroon, D., Lauretano, V., Littler, K., Lourens, L.J., Lyle, M., Pälike, H., Röhl, U., Tian, J., Wilkens, R.H., Wilson, P.A., Zachos, J.C., 2020. An astronomically dated record of Earth's climate and its predictability over the last 66 million years. Science (1979) 369, 1383–1387. https://doi.org/10.1126/science.aba6853

Young, J.R., 1998. Neogene nannofossils. Calcareous Nannofossil Biostratigraphy. British Micropalaeontology Society Publications Series, Cambridge: Kluwer Academic Publisher 225–265.

Young, J.R., Geisen, M., Cros, L., Kleijne, A., Sprengel, C., Probert, I., Østergaard, J., 2003. A guide to extant coccolithophore taxonomy. Journal of Nannoplankton Research Special Issue, 1–132.

Zachariasse, W.J., Gudjonsson, L., Hilgen, F.J., Langereis, C.G., Lourens, L.J., Verhallen, P.J.J.M., Zijderveld, J.D.A., 1990. Late Gauss to Early Matuyama invasions of *Neogloboquadrina Atlantica* in the Mediterranean and associated record of climatic change. Paleoceanography 5, 239–252. https://doi.org/10.1029/PA005i002p00239

Zachariasse, W.J., Jorissen, F.J., Perissoratis, C., Rohling, E.J., Tsapralis, V., 1997. Late Quaternary foraminiferal changes and the nature of sapropel S1 in Skopelos Basin. In Proceedings of the 5th Hellenic symposium on Oceanography and Fisheries, Kavalla, Greece 15–18.

Ziegler, M., Tuenter, E., Lourens, L.J., 2010. The precession phase of the boreal summer monsoon as viewed from the eastern Mediterranean (ODP Site 968). Quat Sci Rev 29, 1481–1490. https://doi.org/10.1016/j.quascirev.2010.03.011

Zijderveld, J.D.A., Hilgen, F.J., Langereis, C.G., Verhallen, P.J.J.M., Zachariasse, W.J., 1991. Integrated magnetostratigraphy and biostratigraphy of the upper Pliocene-lower Pleistocene from the Monte Singa and Crotone areas in Calabria, Italy. Earth Planet Sci Lett 107, 697–714. https://doi.org/10.1016/0012-821X(91)90112-U

Figure captions

Fig. 1. A) Location map of Monte San Nicola section (MSN) and of additional records mentioned in the text; B) Schematic geologic map of Sicily, modified from Radmacher et al. (2023); C) sedimentary profile of the Monte San Nicola type-section with location of the GSSP, sapropel clusters O-C and indication of the interval presented in this study (red dots); D) Stratigraphic log of the investigated interval. A1-A5 indicate sapropel layers belonging to sapropel cluster A, the last cluster of the Piacenzian Stage.

Fig. 2. Main results obtained at Monte San Nicola type-section. From left to right: synthetic stratigraphic log of the section, cumulative abundance of the calcareous nannofossil taxa expressed as percentage, $\delta^{18}O_{G.bulloides}$ record, cumulative abundance of the planktonic foraminifera taxa expressed as percentage.

Fig. 3. Box-and-whisker plot of $\delta^{18}O_{G.bulloides}$ values from MSNt-s (this study) compared with *G. bulloides* and *G. ruber* $\delta^{18}O$ from Mediterranean land sections and deep-sea cores. The horizontal lines show the median, lower and upper margins of the box indicate the 25th and 75th percentiles. The whiskers (the vertical solid lines) indicate the maximum/minimum values. Data of ODP Site 964 from Howell et al. (1998), Singa section from Lourens et al. (1992) and ODP Site 967 from Grant et al. (2022).

Fig. 4. $\delta^{18}O_{G.\ bulloides}$ profile obtained at Monte San Nicola type-section (green line red line represents a 3-points running average) compared with $\delta^{18}O_{G.ruber}$ pattern at the Eastern Mediterranean ODP Site 967 (Grant et al., 2022).

Fig. 5. $\delta^{18}O_{G.\ bulloides}$ record and calcareous plankton climate proxies reconstructed at Monte San Nicola type-section. Colored thicker lines represent a 3-points running average, with the exclusion of the lower resolution profile of PCA1-forams. Yellow bands indicate interglacial phases. Dashed lines trace higher frequency variability during G3 and G1 apparently related to obliquity and insolation forcing. Alkenone-based Mediterranean Sea Surface Temperature record (Herbert et al., 2015, 2018), summer insolation curve 65◦ N and obliquity pattern (Laskar et al., 2004) are also shown for comparison.

Fig. 6. $\delta^{18}O_{G.bulloides}$ profile compared with few calcareous nannofossil taxa showing significant precessional frequencies in their relative abundance as well as the second component of the PCA on the planktonic foraminifera. Yellow bands indicate interglacial phases. The monsoon-run-off proxy and the dry-wet index from Grant et al. (2017) are also shown.

Fig. 7. *N. atlantica* and *U. jafari* percentage abundance with $\delta^{18}O_{G.\ bulloides}$ record at the Monte San Nicola Section. Mediterranean and Atlantic SST, *N. atlantica* abundance from IODP Site U1313 and ice-rafted detritus (IRD) proxies from Site U1313 and ODP Site 984 are shown for correlation.

Fig. 8. $\delta^{18}O_{G.\ bulloides}$ record at Monte San Nicola compared with coeval planktic and benthic $\delta^{18}O$ records from IODP Site U1313 (Bolton et al., 2010) and with the benthic stack record (Lisiecki and Raymo, 2005). Dashed lines indicate analogous shifts in $\delta^{18}O$ patterns.

Tables

Table 1. Loadings of the calcareous nannofossil taxa on the first component (PC1) at the Monte San Nicola Section. The most relevant loadings of PC1 are indicated in red (positive loading) and black bold (negative). The percentage of the variance of the first component is 21%.

Table 2. Loadings of the planktonic foraminifera taxa on the first (PC1) and second component (PC2) at the Monte San Nicola Section. The most relevant loadings of PC1 are indicated in red (positive loading) and black bold (negative). The percentages of the variance of the first and second components are 36% and 26%, respectively.

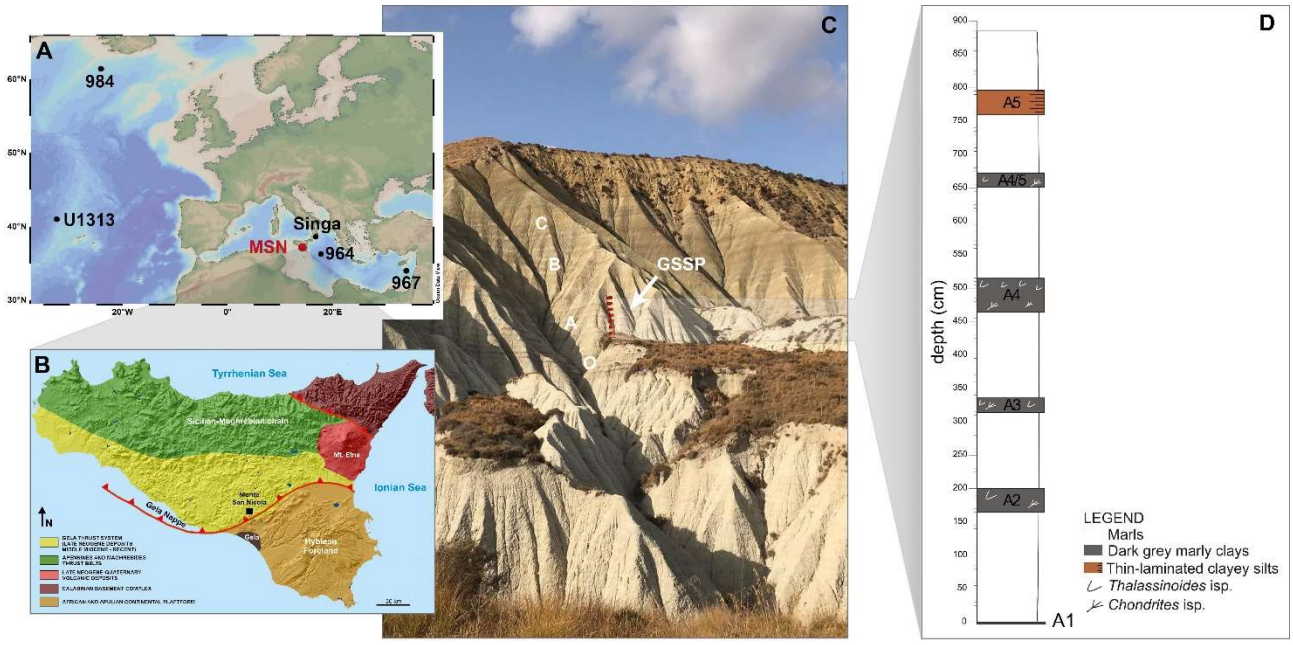
A
984
U1313
Singa
MSN
964
967
60°N
50°N
40°N
30°N
20°W
0°
20°E
B
Tyrrhenian Sea
Sicilian-Maghrebian chain
Mt. Etna
Ionian Sea
Monte San Nicola
Gela Nappe
Gela
Hyblean Foreland
C
GSSP
C
B
A
D
depth (cm)
A5
A4/5
A4
A3
A2
A1
LEGEND
Marls
Dark grey marly clays
Thin-laminated clayey silts
Thalassinoides isp.
Chondrites isp.

Fig. 1

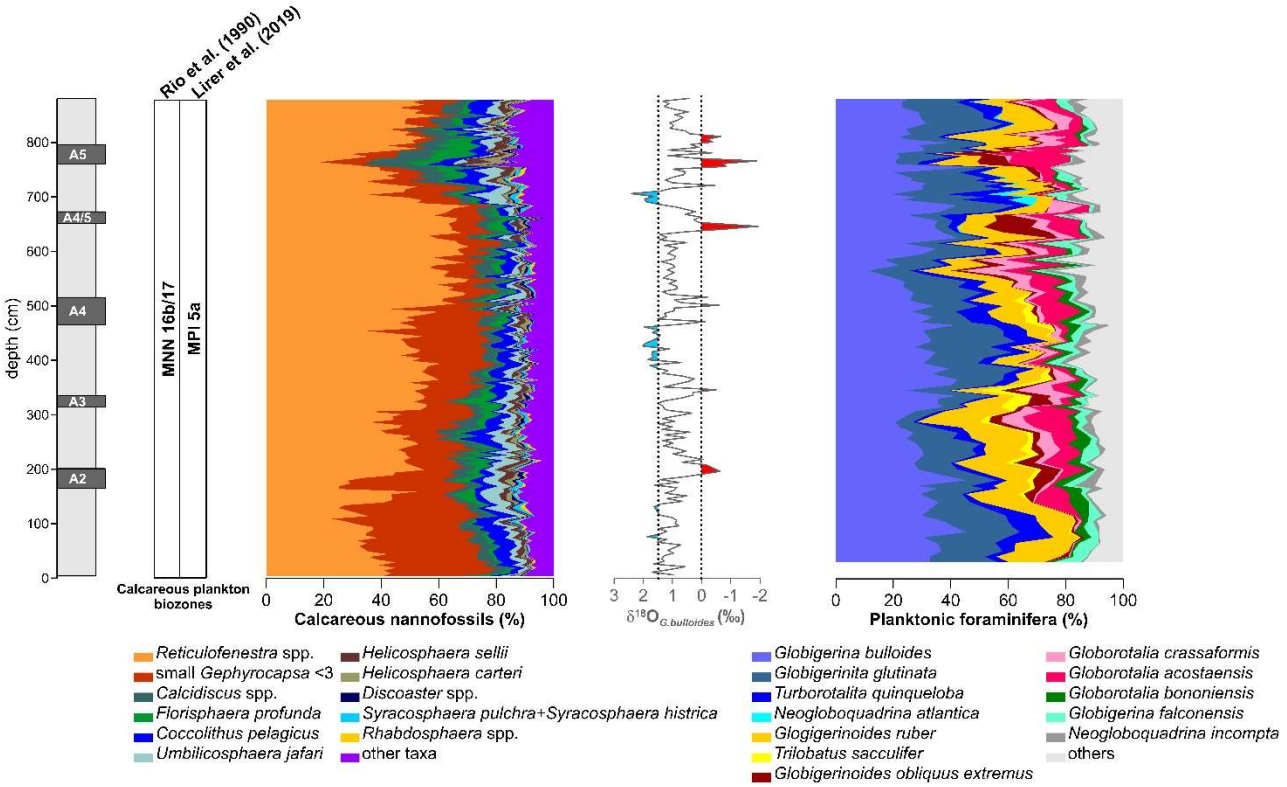
Rio et al. (1990)
Lirer et al. (2019)
depth (cm)
A5
A4/5
A4
A3
A2
MNN 16b/17
MPl 5a
Calcareous plankton biozones
Calcareous nannofossils (%)
δ18OG.bulloides (‰)
Planktonic foraminifera (%)
Reticulofenestra spp.
small Gephyrocapsa <3
Calcidiscus spp.
Florisphaera profunda
Coccolithus pelagicus
Umbilicosphaera jafari
Helicosphaera sellii
Helicosphaera carteri
Discoaster spp.
Syracosphaera pulchra+Syracosphaera histrica
Rhabdosphaera spp.
other taxa
Globigerina bulloides
Globigerinita glutinata
Turborotalita quinqueloba
Neogloboquadrina atlantica
Glogigerinoides ruber
Trilobatus sacculifer
Globigerinoides obliquus extremus
Globorotalia crassaformis
Globorotalia acostaensis
Globorotalia bononiensis
Globigerina falconensis
Neogloboquadrina incompta
others

Fig. 2

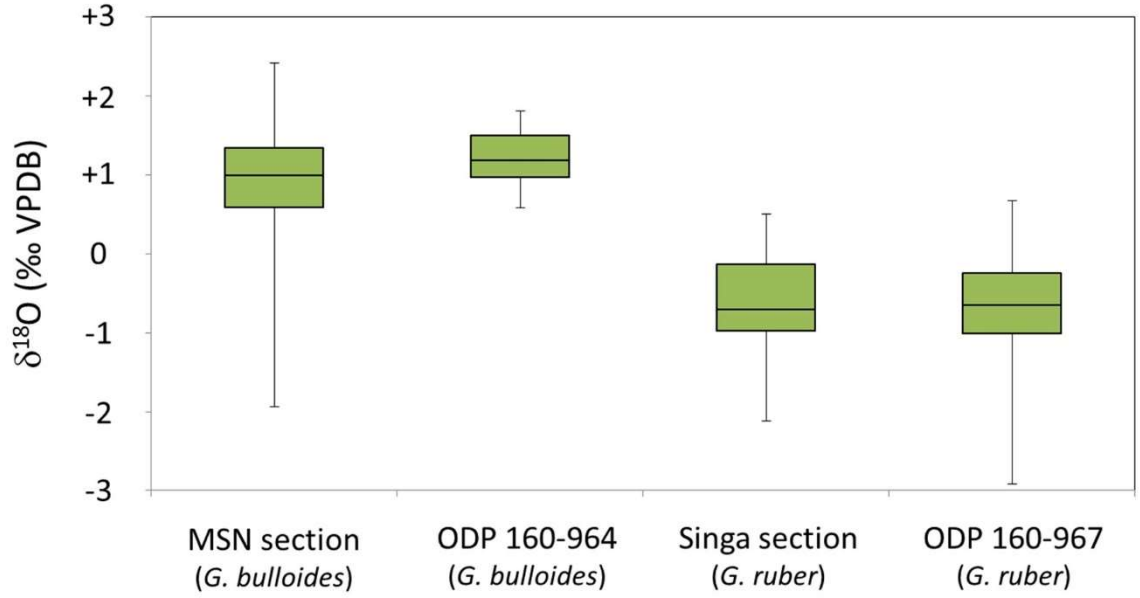
+3
+2
+1
0
-1
-2
-3
δ18O (‰ VPDB)
MSN section
(G. bulloides)
ODP 160-964
(G. bulloides)
Singa section
(G. ruber)
ODP 160-967
(G. ruber)

Fig. 3

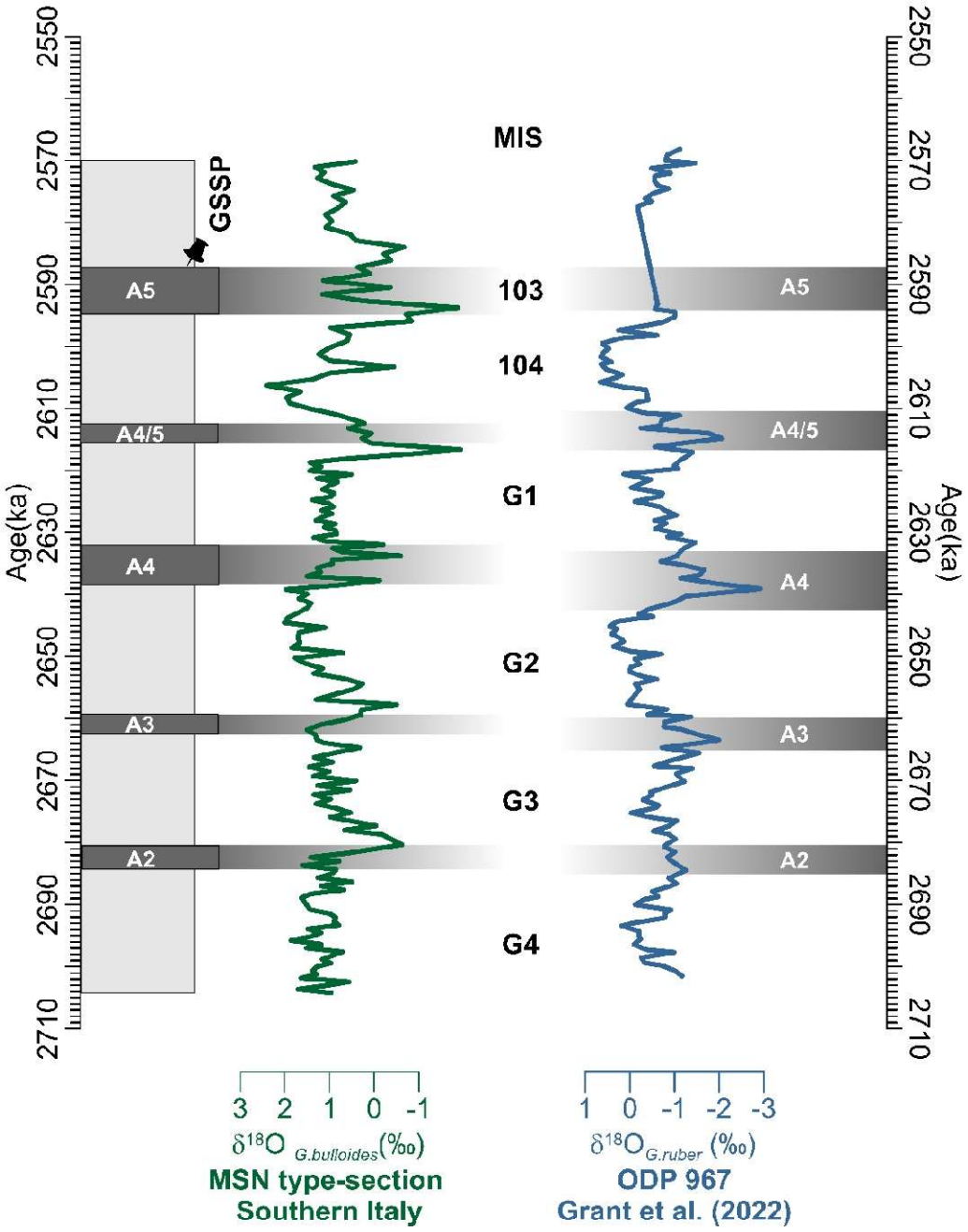
Age(ka)
2550
2570
2590
2610
2630
2650
2670
2690
2710
GSSP
A5
A4/5
A4
A3
A2
MIS
103
104
G1
G2
G3
G4
3 2 1 0 -1
δ18O G.bulloides(‰)
MSN type-section
Southern Italy
1 0 -1 -2 -3
δ18O G.ruber (‰)
ODP 967
Grant et al. (2022)

Fig. 4

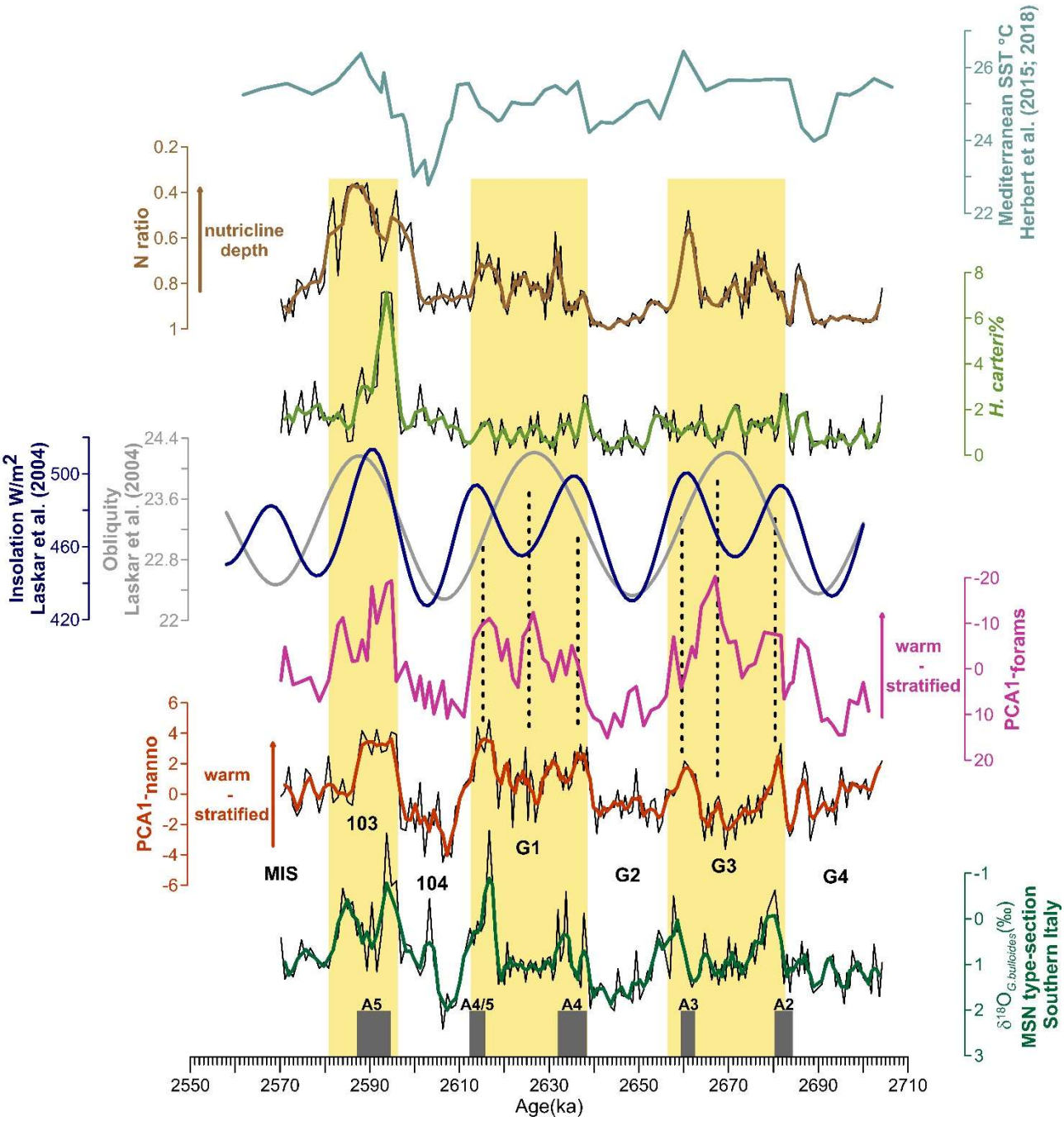
Mediterranean SST °C
Herbert et al. (2015; 2018)
N ratio
nutricline depth
H. carteri%
Insolation W/m2
Laskar et al. (2004)
Obliquity
Laskar et al. (2004)
PCA1-forams
warm - stratified
PCA1-nanno
warm - stratified
MIS
103
104
G1
G2
G3
G4
A5
A4/5
A4
A3
A2
δ18OG.bulloides(‰)
MSN type-section
Southern Italy
Age(ka)

Fig. 5

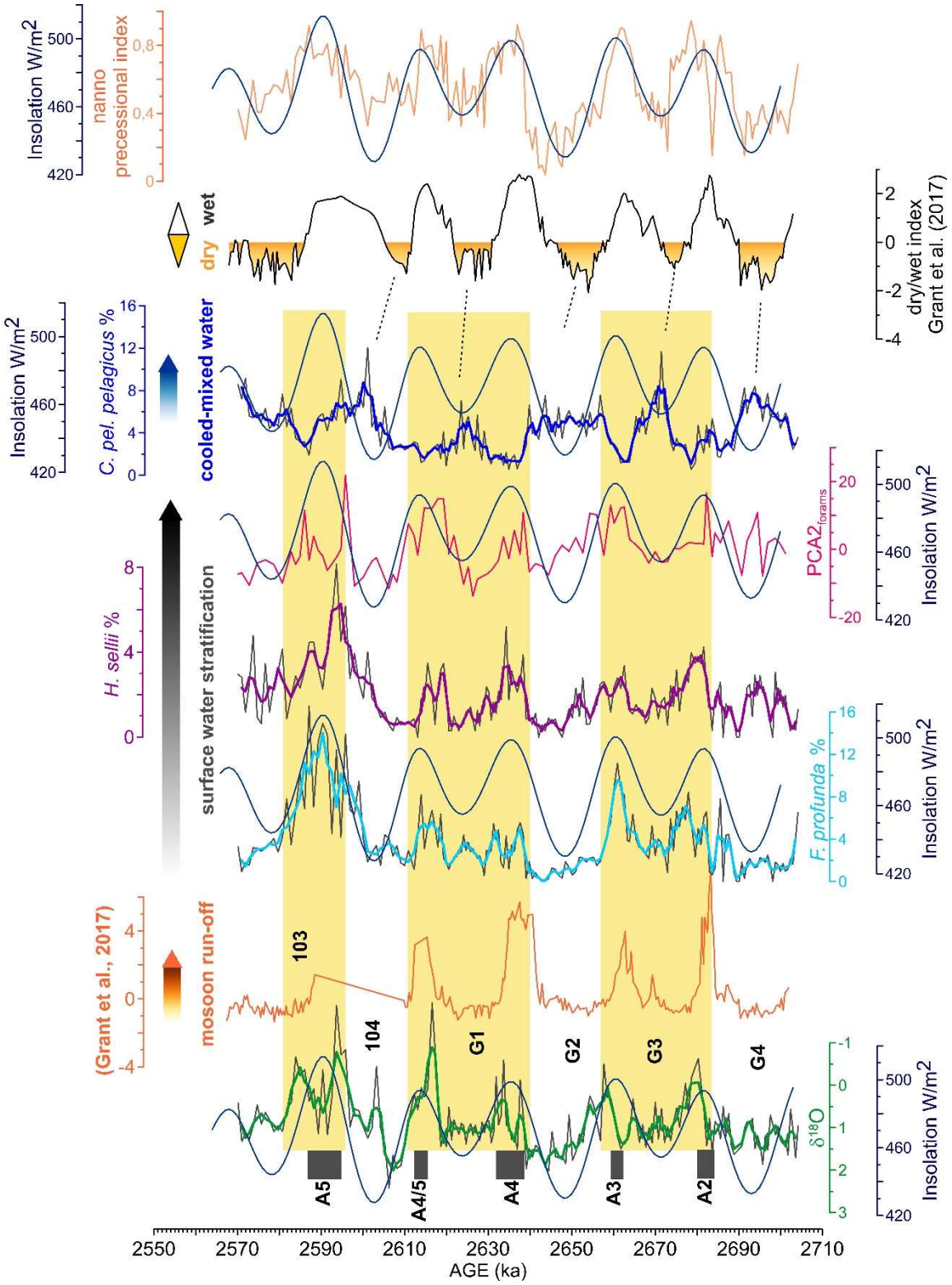
Insolation W/m2
nanno precessional index
wet
dry
dry/wet index Grant et al. (2017)
C. pel. pelagicus %
cooled-mixed water
PCA2foram
H. sellii %
surface water stratification
F. profunda %
(Grant et al., 2017)
mosoon run-off
δ18O
103
104
G1
G2
G3
G4
A5
A4/5
A4
A3
A2
AGE (ka)

Fig. 6

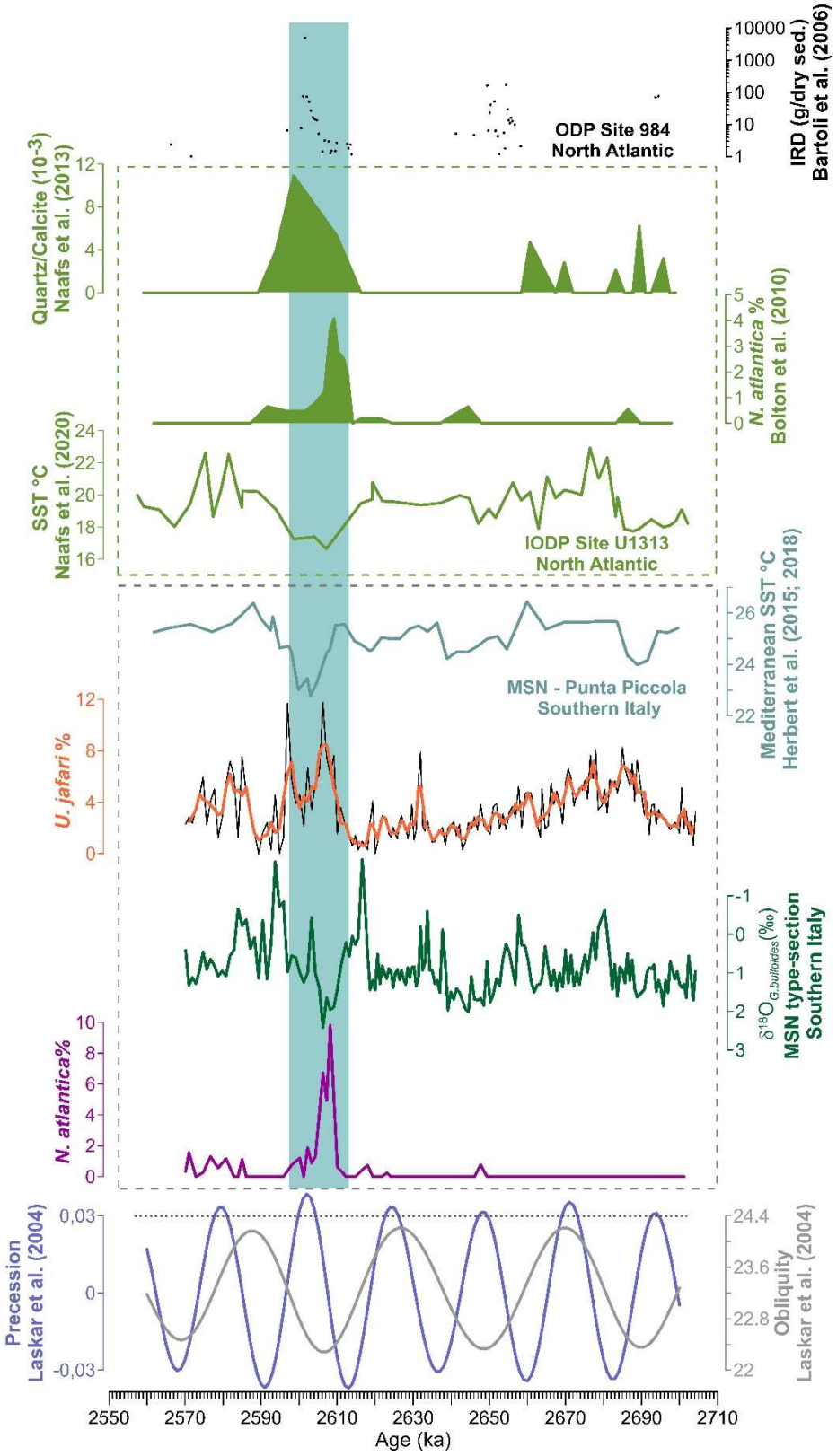
ODP Site 984
North Atlantic
IRD (g/dry sed.)
Bartoli et al. (2006)
Quartz/Calcite (10-3)
Naafs et al. (2013)
N. atlantica %
Bolton et al. (2010)
SST °C
Naafs et al. (2020)
IODP Site U1313
North Atlantic
MSN - Punta Piccola
Southern Italy
Mediterranean SST °C
Herbert et al. (2015; 2018)
U. jafari %
δ18OG.bulloides (‰)
MSN type-section
Southern Italy
N. atlantica%
Precession
Laskar et al. (2004)
Obliquity
Laskar et al. (2004)
Age (ka)

Fig. 7